THE PRESSURE DEPENDENCE OF MUTUAL DIFFUSION IN BINARY GAS MIXTURES

BY

GRAHAM ROBERT STAKER, B.Sc.(HONS.)

A THESIS SUBMITTED FOR THE DEGREE OF

DOCTOR OF PHILOSOPHY

AT THE UNIVERSITY OF ADELAIDE,

MAY, 1976.

Awarded March 1977

DEPARTMENT OF PHYSICAL AND INORGANIC CHEMISTRY.

SUMMARY

Values of the mutual diffusion coefficient, $\mathcal{D}_{12}$, have been measured at 300K over the pressure range of 1-9 atmospheres in binary mixtures of helium with neon, argon, krypton, xenon, nitrogen and carbon dioxide.

Before this study was undertaken, an investigation into the composition dependence of $\mathcal{D}_{12}$ for the helium-nitrogen system was carried out in two groups of diffusion cells. Only one of the two groups yielded mutually consistent results, namely the Loschmidt-type cell, which was subsequently used for the systematic pressure-dependence measurements. It was also generally found that the best results were consistently obtained in the helium-rich composition range. This was believed to be partly due to the reduced occurrence of convection around the matched pair of thermistors used to monitor the diffusion process, by virtue of the high thermal conductivity of helium. The matching of the thermistors in a *helium* environment by the manufacturer was also believed to be a contributing factor.

The results of the pressure dependence study of binary gas mixtures containing 90% helium were compared with the dependence predicted by Thorne's extension to the Enskog theory of transport in dense gases.

I declare that this thesis contains no material accepted for any degree or diploma in any university or institution, and that to the best of my knowledge and belief, it contains no material previously published or written by any other person, except where due reference is made in the text.

ACKNOWLEDGEMENTS

I wish to express my sincerest appreciation to my supervisor, Dr. P.J. Dunlop for his constant guidance and enthusiasm in my work throughout my candidature and for his generous help in collecting data for this project.

To Dr. M.L. Martin and to my colleagues, especially Drs. M.A. Yabsley and P.J. Carson, and Messrs. R.S. Murray and I.R. Shankland, I would like to express my thanks for their interest in my work and for the useful discussions we have had from time to time.

Also, I would like to thank Messrs. K. Shepherdson and J. Beard, of the Electronics Workshop and Mr. A. Bowers and other members of the Mechanical Workshop for their able assistance.

For their parts in the proof-reading of the manuscript I am grateful once again to Dr. Dunlop and to my wife, Therese, who singled out the phrases discordant to her.

I would like to commend Mrs. D. Darwent and Mrs. J. Tieste for their patient interpretation of the manuscript into type, and my father for his critical perusal of the finished copy.

Finally, I would like to dedicate this thesis to my wife whose moral support during this period was invaluable to me.

TABLE OF CONTENTS

TABLE OF CONTENTS (cont'd.)

TABLE OF CONTENTS (cont'd.)

LIST OF TABLES

LIST OF TABLES (cont'd.)

LIST OF FIGURES

CHAPTER 1

GENERAL INTRODUCTION

1.1 *EXPERIMENTAL*

In recent years there has been a wealth of data published on the mutual diffusion of gases in dilute binary mixtures, the bulk of which has been reviewed and critically evaluated by Marrero and Mason[1]. This compilation does not include the more recent data measured in this laboratory, in which very precise absolute values of binary diffusion coefficients $\mathcal{D}_{12}$ have been claimed (see Chapter 3, Refs. 5-13), using pairs of matched thermistors as concentration-sensing devices.

On the other hand there seems to be very little data available on the pressure (or density) dependence of diffusion in mixtures. This scarcity, plus the high precision attainable with the apparatus in this laboratory, was the motivation for this project.

In spite of the precision claimed earlier, it was found that there was still a significant uncertainty in the absolute value of $\mathcal{D}_{12}$ due to the disagreement between different cells used in this laboratory. Part of this project was to investigate this apparent cell-dependence with the view to eliminating such ambiguity. These experiments are described in Chapter 4.

Thermistors have been in common use for some years as

sensing devices in gas chromatography. Their recent application in the monitoring of diffusion[2,3] obviates the necessity of withdrawing samples for analysis. The method for measuring $\mathcal{D}_{12}$ in this laboratory using thermistors is outlined in Chapter 3. A disadvantage of using thermistors as composition detectors is that their operating temperatures must be above that of the surrounding gas, hence the problem of convection arises. This becomes more acute, both as the density of the gas increases and, if the composition of the gas is changing, as the thermal conductivity of the gas decreases. Attempts to determine a composition dependence of the product $p\mathcal{D}_{12}$ over a range of pressures, p, were unsuccessful partly for this reason. As will be explained in Chapter 5, all pressure-dependence measurements were subsequently confined to mixtures containing 90% helium.

1.2 *THEORETICAL*

A theory of transport in dense gases was developed by Enskog as an extension to the Chapman-Enskog theory of dilute gases[4-6]. His theory, derived for a hypothetical gas composed of rigid spheres, was based on a modification of the Boltzmann equation by the insertion of a factor, Y, dependent on the rigid sphere diameter and the number density, n, which accounted for the change in collision frequency of the molecules on compression of the gas. This factor is commonly identified with the value of the equilibrium radial distribution function at the point of contact of the colliding spheres. As in the dilute gas theory, it is assumed that only binary collisions occur. H.H. Thorne[5] generalised Enskog's theory to binary mixtures

of hard spheres. His extension, as applied to the density dependence of binary diffusion in gases, was tested against the data obtained in this project.

General theories of the density dependence of transport coefficients, in various states of development, have been comprehensively reviewed by Brush[7]. In one approach, a set of equations involving successively higher order distribution functions (the BBGKY hierarchy, named after the co-founders of the theory, Bogoliubov, Born, Green, Kirkwood and Yvon) is derived from the Liouville equation, and a generalised Boltzmann equation may be obtained from the first equation in this set[8]. This approach has been the starting point for the derivation of density expansions for the transport coefficients in analogy to the virial equation of state. Expressions for the first density corrections to the transport properties in binary mixtures have been given by Bennett and Curtiss[9]. These expressions, containing collisional transfer and 3-body contributions, are functionals of an arbitrary potential function but are strictly applicable only to repulsive potentials because, as with the theory developed for single-component gases[10], bound states are not considered. For this reason, the best agreement with experiments is expected at high reduced temperatures.

Stogryn and Hirschfelder[11] and Kim and Ross[12] have developed approximate theories applicable at low reduced temperatures to account for the interaction between monomers and dimers in the density dependence of viscosity. Wakeham[13] has carried over Stogryn's approach to the

estimation of the effect of these interactions on the density dependence of self and mutual diffusion. This theory, however, is difficult to apply to binary systems unless one component is present in trace amounts.

In the next chapter, some of the background theory of gaseous diffusion is reviewed in relation to binary mixtures of real gases. Where numbered subscripts are used on symbols, the convention used here is that 2 denotes the heavier component.

REFERENCES

1 T.F. Marrero and E.A. Mason, J. Phys. Chem. Ref. Data 1 3 (1972).

2 R.R.J. Van Heijningen, A. Feberwee, A. Van Oosten and J.J.M. Beenakker, Physica 32 1649 (1966).

3 R.R.J. Van Heijningen, J.P. Harpe, and J.J.M. Beenakker, Physica 38 1 (1969).

4 D. Enskog, Kungl. Svenska Vetenskaps Akademiens Handl., 63 (1922).

5 S. Chapman and T.G. Cowling, "The mathematical theory of non-uniform gases", (3rd ed.), Cambridge U.P. (1970).

6 J.O. Hirschfelder, C.F. Curtiss and R.B. Bird, "Molecular theory of gases and liquids", (4th printing) Wiley (1964).

7 S.G. Brush, "Kinetic theory", (Vol. 3), Pergamon Press (1972).

8 N.N. Bogoliubov, J. Phys. (U.S.S.R.) 10 265 1946; also "Studies in statistical mechanics", I, North Holland Pub. Co. (1962).

9 D.E. Bennett and C.F. Curtiss, J. Chem. Phys. 51 2811 (1969).

10 D.K. Hoffman and C.F. Curtiss, Phys. Fluids, 8 890 (1965).

11 D.E. Stogryn and J.O. Hirschfelder, J. Chem. Phys. 31 1531 (1959).

12 S.K. Kim and J. Ross, J. Chem. Phys. 42 263 (1965).

13 W.A. Wakeham, J. Phys. B. 6, 372 (1973).

CHAPTER 2

THEORY OF GASEOUS DIFFUSION

2.1 *INTRODUCTION*

In this chapter a review is made of some of the main theoretical aspects of gaseous diffusion relevant to this work. Firstly, a discussion of the macroscopic process of diffusion is given, followed by the kinetic theory approach of Chapman and Enskog to diffusion in dilute gases. The extension of this theory to moderately dense single component gases by Enskog and the further extension of the theory by Thorne to include binary mixtures, is presented at the end of the chapter.

2.2 *PHENOMENOLOGICAL THEORY*

Diffusion may be defined as the macroscopic flow of a chemical species relative to other species in the system, the flow being produced by some gradient within the system or by the influence of some external force. In a gaseous system at constant temperature and pressure and in the absence of any external forces, diffusion can only take place if there is a concentration gradient. The flow of matter takes place in such a direction that the components of the system become uniformly distributed. Under these conditions the process is called isothermal diffusion. This term is strictly a misnomer because in reality the transport of matter even in an ideal system is associated

with the transport of energy. The production of a temperature gradient in a system in this manner is known as the Dufour[1] effect and is the converse phenomenon to thermal diffusion[2] which is the flow of matter under the influence of a temperature gradient, resulting in the partial segregation of the components of an initially uniform mixture. Both effects, being second order in nature, cannot be satisfactorily explained by elementary kinetic theory; on the other hand, these phenomena are predicted as a consequence of the rigour of the Chapman-Enskog theory[3]. In addition to these effects, transport of matter produces a pressure gradient; however, this is negligible except in the case of diffusion along a capillary[4].

For a two-component system close to equilibrium, the flux of each species is directly proportional to the concentration gradient producing it. This is a statement of Fick's first law of diffusion[5]. If the fluxes are measured relative to the local centre-of-volume of the system, the two fluxes conform to the relationship,

$$\sum_{i=1}^{2} V_i \underset{\sim}{j}_i^v = 0, \qquad (2.1)$$

where $\underset{\sim}{j}_i^v$ is the mole flux vector of species i at right angles to a unit cross section moving at the same velocity as the *local centre-of-volume* of the system, and the partial molar volume, $\overline{V}_i$ of species i is defined as

$$\overline{V}_i = (\partial V / \partial n_i)_{n_j}, \qquad (j \neq i). \qquad (2.2)$$

Fick's law may then be expressed for this system as

$$-\underset{\sim}{j}_i^v = D_i^v \nabla c_i, \quad i=1,2, \tag{2.3}$$

where ∇c_i is the gradient in concentration of the i^{th} species at constant temperature and pressure, and D_i^v is the proportionality constant. It can easily be shown, using Eq. (2.1) and the thermodynamic relationship,

$$\sum_{i=1}^{m} c_i \bar{V}_i = 1 \quad \text{(m components)}, \tag{2.4}$$

that

$$D_1^v = D_2^v \equiv \mathcal{D}_{12}, \tag{2.5}$$

where $\mathcal{D}_{12}$ is the binary diffusion coefficient for the system.

Eqs. (2.3) may be generalised to systems containing more than two components:

$$-\underset{\sim}{j}_i^v = \sum_{k=1}^{m} D_{ik}^v \nabla c_k, \quad i=1,2,\ldots m, \tag{2.6}$$

where the D_{ik}^v are called the multicomponent diffusion coefficients. These systems will not be considered any further.

On combining the equation of continuity for a chemically inert system[6],

$$\partial c_i/\partial t + \nabla . \underset{\sim}{j}_i^v = 0, \tag{2.7}$$

with Eq. (2.3), one obtains a mathematical statement of Fick's second law of diffusion:

$$\partial c_i/\partial t = \nabla . (\mathcal{D}_{12} \nabla c_i), \quad i=1,2. \tag{2.8}$$

If diffusion is restricted to one dimension, say the

z direction, and it is assumed that $\mathcal{D}_{12}$ is negligibly dependent upon concentration, Eq. (2.8) becomes:

$$(\partial c_i/\partial t) = \mathcal{D}_{12}(\partial^2 c_i/\partial z^2). \qquad (2.9)$$

In actual fact $\mathcal{D}_{12}$ is slightly concentration dependent (of the order of 2.5% over the composition range for helium-nitrogen) but Ljunggren[7] has shown that the measured diffusion coefficient corresponds to the mean concentration at the end of the experiment if the concentration varies *linearly* during the run. This condition will be met if the system is not far removed from equilibrium when measurements are made. Eq. (2.9) is a standard second order partial differential equation which lends itself readily to solution by standard methods[8] subject to the appropriate boundary and initial conditions. The solution is a concentration distribution function which varies with time at a rate related to the diffusion coefficient.

2.3 *DIFFUSION IN REAL GAS MIXTURES*

As we have just mentioned, isothermal diffusion is a misnomer, even in ideal gases. When two unlike real gases mix there is an additional contribution to the temperature disturbance due to the heat of mixing effect. The magnitude of this effect may be estimated from a knowledge of the equation of state for the mixture, which in moderately dense gases is adequately represented by the first two terms of the virial expansion[9]

$$p\bar{V}/RT = 1+B'_m(T)p+ \ldots., \qquad (2.10)$$

assuming only *binary* collisions occur. $B'_m(T)$ is the *second*

pressure virial coefficient of the mixture and is related simply to the virial coefficients of components 1 and 2 and of the interaction between 1 and 2 by

$$B'_m = \sum_{i=1}^{2} \sum_{j=1}^{2} x_i x_j B'_{ij}, \qquad (2.11)$$

where $x_i (= 1-x_j)$ is the mole fraction of species i in the two-component system. $\overline{V}$ in Eq. (2.10) is the molar volume of the mixture, p is the total pressure, T is the absolute temperature and R is the gas constant. A knowledge of the temperature dependence of the second virial coefficient gives some insight into bimolecular interactions[10].

The heat of mixing of two gases at moderate densities is given approximately by[11]

$$\overline{H}^E = \overline{H}-\overline{H}^{ideal} = -2x_1x_2RT^2p(dE'/dT) \qquad (2.12)$$

where $\overline{H}^E$ is the excess molar enthalpy of mixing ($\overline{H}^{ideal} = 0$) and E' is the excess second pressure virial coefficient, defined by

$$E' = B'_{12}-\tfrac{1}{2}(B'_{11}+B'_{22}). \qquad (2.13)$$

This effect will obviously be maximised when equal quantities of the two gases interdiffuse to give a 50/50 mixture. To minimise the interference from the heat of mixing in diffusion experiments it is therefore preferable to work at mole fractions close to zero or unity.

A companion effect to the heat of mixing of two gases in a closed volume is the pressure of mixing. This results in the final pressure of the mixture being different from the average pressure of the separated components. In a

Loschmidt type diffusion cell[12] this effect can be quite significant especially when two pure unlike gases diffuse into each other. This can lead to a large uncertainty in the diffusion coefficient which depends approximately on the inverse of the pressure. It is not easy to measure the pressure change precisely; however an estimate can be obtained by using Eq. (A.7) in Appendix A. This equation predicts that for the system helium-xenon *at 10 atmospheres pressure*, the pressure change amounts to about +1.8% when equal volumes of pure helium and of pure xenon diffuse into each other. If, however, a mixture of 80% helium with xenon interdiffuses with the same volume of pure helium, the resulting pressure increment is only 0.07%, which is of the order of experimental uncertainty in the pressure. A similar magnitude is predicted for the case of pure xenon and a mixture of 80% xenon and 20% helium. It will be shown in a later chapter that this is only one of several reasons for choosing to carry out Loschmidt cell experiments within the composition range in which helium is in excess.

We shall now consider the other phenomenon which disturbs the temperature equilibrium during "isothermal" diffusion, namely the Dufour effect. When a concentration gradient exists in a mixture of two unlike gases, whether they be real or ideal, there exists an associated temperature gradient which acts to retard the mixing process. The theory of the effect predicts that the lighter gas is heated and the heavier gas is cooled. Experimental observations confirm this[13,14], but demonstrate that the maximum heating and cooling effects are generally unequal.

This is attributed to the superimposition of the heat of mixing effect[14] which we have just discussed.

Both temperature effects have been characterised mathematically in a single equation derived by Ljunggren[7]. The two contributions to the initial temperature transient decay at different rates. Ljunggren has shown that the Dufour effect decays at approximately the same rate as the ordinary diffusion process, whereas it has been deduced[15] that the heat of mixing effect decays roughly three times as fast.

2.4 *THE CHAPMAN-ENSKOG THEORY OF DILUTE GASES*

A classical-mechanical analysis of the time evolution of a large system of particles ultimately leads to the problem of solving the Boltzmann integro-differential equation[16]:

$$\hat{D}_i f_i = \sum_j J(f_i, f_j) \qquad (2.14)$$

where $\hat{D}_i$ is a differential operator defined by

$$\hat{D}_i = \partial/\partial t + \underset{\sim}{v}_i \cdot \nabla \qquad (2.15)$$

which incorporates the streaming operator $\underset{\sim}{v}_i \cdot \nabla$. $J(f_i, f_j)$ is a triple integral related to the dynamics of a bimolecular collision between species i and j, and f_i is the velocity distribution function of species i which is defined as the average number of molecules of the i^{th} species to be found at a particular time t in a unit volume centred at position $\underset{\sim}{r}$ from the origin and moving within a unit range of velocities about $\underset{\sim}{v}_i$. At equilibrium,

the solution to Eq. (2.14) is the Maxwell-Boltzmann distribution function,

$$f_i^{(0)} = n_i(m_i/2\pi kT)^{3/2}\exp(-m_i v_i^2/2kT), \qquad (2.16)$$

where n_i and m_i are the number density and molecular mass respectively of species i, and k is Boltzmann's constant.

Non-equilibrium solutions to (2.14) may be obtained by the Chapman-Enskog approach which is applicable to systems not too far removed from equilibrium. This approach is essentially a perturbation method which assumes that the non-equilibrium solution is equal to the Maxwell-Boltzmann distribution plus a small perturbation term which decays to zero as the system tends towards equilibrium, that is

$$f_i \simeq f_i^{(0)}(1+\psi_i) \qquad (2.17)$$

where ψ_i is the perturbation function which is directly proportional to the gradients in the system. The perturbation procedure leads to an equation similar in form to Eq. (2.14) with f_i replaced by $f_i^{(0)}$ on the left hand side, and a modified integral containing $f_i^{(0)}$ and the unknown function, ψ_i on the right hand side. The "linearised" Boltzmann equation can be solved for ψ_i by a variational technique[17] or by the solution of an infinite set of linear equations[3]. Both methods employ Sonine polynomials[3] which appear in the coefficients of the gradients. Having determined ψ_i and hence the distribution function to the order of the first perturbation, the transport coefficients can be calculated by integrating the distribution function

to obtain the appropriate flux vectors. If the second method is used, the exact values of the transport coefficients are obtained in principle from the ratio of two infinite determinants. Fortunately in practice these may be approximated adequately by finite determinants. Different truncation schemes used by Chapman and Cowling[3] and by Kihara[18] converge very rapidly for the diffusion coefficient[19]. The first approximation to the diffusion coefficient is obtained by considering only the first term of the Sonine expansion. Both methods give

$$n\,[\mathcal{D}_{12}]_1 = \frac{3}{8}(kT/2\pi\mu_{12})^{\frac{1}{2}}/\sigma_{12}^2\Omega_{12}^{(1,1)*}(T^*), \qquad (2.18)$$

where $[\cdots]_m$ symbolises the m^{th} approximation, μ_{12} is the reduced molecular mass $m_1m_2/(m_1+m_2)$ of species 1 and 2 and n is the total number density. T^* is a reduced temperature, equal to kT/ε_{12} where ε_{12} is the depth of the potential energy well for the encounter between two unlike molecules. $\Omega_{12}^{(1,1)*}$ is a universal function of T^*, which has been tabulated[10] for various potential energy functions $\phi(r)$, including the widely used Lennard-Jones (m,6) function,

$$\phi_{L.J.}(r) = \varepsilon\,[m/(m-6)]\,(m/6)^{6/(m-6)}\,[(\sigma/r)^m - \sigma/r)^6]. \qquad (2.19)$$

Here, r is the internuclear separation, σ is a measure of molecular size, taken to be the internuclear distance at which $\phi_{L.J.}(r) = 0$, and m is a measure of the strength of the repulsive force between the molecules and is commonly assigned the value of 12. $\Omega^{(1,1)*}$ is actually a *ratio* obtained by dividing the *collision integral* $\Omega^{(1,1)}$, a

functional of $\phi(r)$, by the corresponding integral calculated on the basis of the rigid elastic spheres model:

$$\phi_{R.S.}(r) = \infty \text{ if } r \leqslant \sigma, \text{ or } 0 \text{ if } r > \sigma. \qquad (2.20)$$

The collision integrals $\Omega^{(l,s)}$ are related to the Sonine expansion coefficients, and in reduced form are useful for the calculation of intermolecular force parameters from the transport properties and vice-versa. They also provide a measure of the departure of the molecular dynamics from rigid spheres behaviour at a particular temperature. By definition $\Omega^{(l,s)*}$ for rigid spheres gases is identically equal to unity.

It is notable that to the first approximation (Eq. (2.18)) binary diffusion coefficients depend only on interactions between unlike molecules, thus diffusion measurements provide a useful tool for studying such interactions. At this level of approximation the theoretical diffusion coefficient is independent of composition. It can also be seen from Eq. (2.18) that for a particular system at constant temperature, the product $n[\mathcal{D}_{12}]_1$ is invariant with number density and hence with pressure.

Higher approximations to the diffusion coefficient can be calculated by using more terms in the Sonine expansion. The Kihara second approximation (two terms of the expansion) is given by[20]

$$n[\mathcal{D}_{12}]_2 = n[\mathcal{D}_{12}]_1 (1+\Delta'). \qquad (2.21)$$

where

$$\Delta' = 0.1(6C_{12}-5)^2(x_1^2P_1+x_1x_2P_{12}+x_2^2P_2)/(x_1^2Q_1^*+x_1x_2Q_{12}^*+x_2^2Q_2^*) \qquad (2.22)$$

where x_i are the mole fractions of the two components. If M_i are the molecular weights and we define the quantities

$$Z_1 = M_1/(M_1+M_2) \tag{2.23}$$

and

$$F_1 = (\Omega_{11}^{(2,2)*}\sigma_{11}^2)/(\Omega_{12}^{(1,1)*}\sigma_{12}^2) \tag{2.24}$$

with similar definitions for Z_2 and F_2 by interchange of subscripts, then the coefficients in Eq. (2.22) are given by

$$\begin{aligned} P_1 &= (2Z_1M_1/M_2)(2Z_2)^{\frac{1}{2}}F_1 \\ P_{12} &= 15(Z_1-Z_2)^2+8Z_1Z_2A_{12}^* \\ Q_1' &= (2Z_1M_1/M_2+6Z_2+3.2Z_1A_{12}^*)(2Z)^{\frac{1}{2}}F_1 \\ Q_{12}' &= 15(Z_1-Z_2)^2+32Z_1Z_2A_{12}^*+1.6(Z_1Z_2)^{-\frac{1}{2}}F_1F_2. \end{aligned} \tag{2.25}$$

P_2 and Q_2' are similarly obtained by interchange of subscripts 1 and 2. A_{12}^* and C_{12}^* are ratios of collision integrals defined by

$$\begin{aligned} A_{12}^* &= \Omega_{12}^{(2,2)*}/\Omega_{12}^{(1,1)*} \\ \text{and} \quad C_{12}^* &= \Omega_{12}^{(1,2)*}/\Omega_{12}^{(1,1)*}. \end{aligned} \tag{2.26}$$

As Mason has shown[19] it is rarely necessary to make calculations beyond the Kihara second approximation unless high precision warrants it. In one such case Yabsley[21] has calculated the Lennard-Jones (12,6) potential parameters ϵ_{12}/k and σ_{12} by comparing precise binary diffusion data for five noble gas mixtures with the Chapman-Cowling *fourth* approximation to the diffusion coefficients.

We conclude this section by summarising some of the

main assumptions inherent in the Chapman-Enskog theory of dilute gases[10]:-

(i) The size of the molecules is negligible compared with the average distance between them. In the collision term of the Boltzmann equation (2.14) the distribution functions of the colliding species are evaluated about the same position $\underset{\sim}{r}$ at the moment of contact.

(ii) Only *binary* collisions occur. It is assumed that the occurrence of ternary and higher order collisions is negligible in dilute gases.

(iii) The collisions are *elastic*, that is the molecules possess no internal degrees of freedom. Strictly this requirement limits the theory to spherical molecules; however, the coefficients of diffusion and viscosity are not affected greatly if this requirement is relaxed to include polyatomic molecules, provided they do not deviate too much from spherical symmetry.

(iv) The mean free path is negligible compared with the dimensions of the container, thus the gas behaves as a continuum. The theory does not apply to systems which are so dilute that a significant percentage of the collisions takes place between the gas molecules and the walls of the container. A *Knudsen* gas is an extreme case where gas-wall collisions predominate.

(v) The system is not far removed from equilibrium. Consequently, the fluxes in the macroscopic properties of the system are directly proportional to the gradients producing them. Under such circumstances the system obeys the Navier-Stokes equations of change. These

equations are non-applicable only when extremely large gradients exist at normal pressures, as in shock waves. If the system is extremely dilute, deviations from Navier-Stokes behaviour may occur with much smaller gradients.

(vi) Classical mechanics generally gives an adequate description of the dynamics of the system; however, at low temperatures, corrections must be made for the wave nature of the light molecules, particularly the isotopes of hydrogen and helium. The only change to the formulae for the transport coefficients occurs in the collision integrals which are evaluated in terms of phase-shifts instead of angles of deflection. These quantum-corrected collision integrals have been evaluated for the Lennard-Jones (12,6) potential[30,31].

2.5 *EXTENSION TO MODERATELY DENSE GASES*

In conflict with experimental observation the Chapman-Enskog theory predicts that the product $n\mathcal{D}_{12}$ does not vary with number density, n. Enskog[3] modified the theory to take into account the finite size of the molecules; however the assumption of binary collisions was retained. For the sake of simplicity he considered a pure gas composed of rigid elastic spherical molecules, and introduced a quantity Y, dependent only on n for that gas, which represented the factor by which the collision frequency differed from that of a gas composed of point particles on compression.

The function Y, related to the equation of state for rigid spheres gases,

$$p = nkT(1+\frac{2}{3}n\pi\sigma^3 Y), \tag{2.27}$$

is made up of two contributions, the first of which tends to decrease the collision frequency due to the shielding effect of the finite-sized molecules and the second, over-riding the first, increases the collision frequency due to the closer proximity of the molecules when the gas is compressed.

The modified Boltzmann equation incorporates in the collision term the factor Y which is evaluated at the point of impact of the colliding spheres. The corresponding distribution functions of the colliding molecules are distinguished by the finite separation σ of the centres of the molecules upon impact. For self-diffusion the Enskog rigid spheres density dependence is

$$n\mathcal{D} = (n\mathcal{D})_0/Y, \tag{2.28}$$

where $(n\mathcal{D})_0$ is the dilute gas value of the product and Y is given by

$$Y = 1 + \frac{5}{12}n\pi\sigma^3 + \mathcal{O}(n^2). \tag{2.29}$$

Enskog's theory was generalised to binary mixtures by Thorne[3]. The density dependence of mutual diffusion is given by

$$n\mathcal{D}_{12} = (n\mathcal{D}_{12})_0 Y_{12}^{-1}[1+n\pi x_1 x_2(\sigma_{22}-\sigma_{11})^2(\sigma_{22}+\sigma_{11})] \tag{2.30}$$

where

$$Y_{12} = 1+(2n\pi/3)[x_1\sigma_{11}^3\xi+x_2\sigma_{22}^3(5/4-\xi)]+\mathcal{O}(n^2) \tag{2.31}$$

and

$$\xi = (\sigma_{11}+4\sigma_{22})/(4\sigma_{11}+4\sigma_{22})$$

The term [1+...] in Eq. (2.30) is the rigid spheres expression for the non-ideality factor $(\partial \ln a_1/\partial \ln x_1)_{T,p}$[22,23]. It is derived in Appendix B using Guggenheim's expression for the absolute activity a_i of species i in a slightly imperfect gas mixture[24].

Eq. (2.30) may be rearranged to express the density dependence in the form[25]

$$n\mathcal{D}_{12} = (n\mathcal{D}_{12})_0 [1+B^{r.s.}n] \qquad (2.32)$$

where

$$B^{r.s.} = \pi x_1 x_2 (\sigma_{22}-\sigma_{11})^2(\sigma_{22}+\sigma_{11}) - (2\pi/3)[x_1\sigma_{11}^3\xi + x_2\sigma_{22}^3(5/4-\xi)]. \qquad (2.33)$$

$B^{r.s.}$ may be regarded as a rigid spheres density "virial coefficient" for mutual diffusion. Eq. (2.32) is in a convenient form for comparison of the theoretical and experimental density dependences of diffusion in binary gas mixtures at moderate densities.

It has recently been demonstrated[26,27] that Thorne's equations are inconsistent with irreversible thermodynamics, however the modifications proposed only affect terms which are second order or higher in number density[28,29].

REFERENCES

1 L. Dufour, Pogg. Ann. 148 490 (1873).

2 S. Chapman and F.W. Dootson, Phil. Mag. 33 248 (1917).

3 S. Chapman and T.G. Cowling, "The mathematical theory of non-uniform gases", 3rd ed. Cambridge U.P. (1970).

4 K.P. McCarty and E.A. Mason, Phys. Fluids, 3 908 (1960).

5 A. Fick, Ann. Physik, U. Chem. 94 59 (1855).

6 D.D. Fitts, "Non-equilibrium thermodynamics", McGraw-Hill (1962).

7. S. Ljunggren, Ark. Kemi. 24 1 (1965).

8 For example, H.S. Carslaw and J.C. Jaeger, "Conduction of heat in solids", Oxford University Press (1947).

9 H. Kamerlingh Onnes, Commun. Phys. Lab. Univ. Leiden, No. 71 (1901).

10 J.O. Hirschfelder, C.F. Curtiss and R.B. Bird, "The molecular theory of gases and liquids", (4th printing) Wiley (1964).

11 M. Knoester, K.W. Taconis and J.J.M. Beenakker, Physica, 33 389 (1967).

12 J. Loschmidt, Sitzber. Akad. Wiss. Wein, 61 367 (1870).

13 K. Clusius and L. Waldmann, Die Naturwissenschaften, 30 711 (1942).

14 L. Miller, Z. Naturforsch, 4a 262 (1949).

15 M.A. Yabsley, Ph.D. thesis, University of Adelaide, (1975).

16 L. Boltzmann, Wein Sitz. 66 275 (1872).

17 C.F. Curtiss and J.O. Hirschfelder, J. Chem. Phys. 17 550 (1949).

18 T. Kihara, Revs. Modern Phys. 25 831 (1953).

19 E.A. Mason, J. Chem. Phys. 27 782 (1957).

20 E.A. Mason, J. Chem. Phys. 27 75 (1957).

21 G.R. Staker, M.A. Yabsley, J.M. Symons and P.J. Dunlop, J. Chem. Soc., Faraday Trans. I., 70 825 (1974).

22 D.C. Douglass and H.L. Frisch, J. Phys. Chem. 73 3039 (1969).

23 M.K. Tham and K.E. Gubbins, J. Chem. Phys. 55 268 (1971).

24 E.A. Guggenheim, "Thermodynamics", 2nd ed., Nth. Holland Pub. Co. (1950).

25 D.E. Bennett and C.F. Curtiss, J. Chem. Phys. 51 2811 (1969).

26 L. Barajas, L.S. García-Colin and E. Piña, J. Stat. Phys. 7 161 (1973).

27 H. Van Beijeren and M.H. Ernst, Physica, 68 437 (1973).

28 E. Piña, J. Stat. Phys. 11 433 (1974).

29 H. Van Beijeren and M.H. Ernst, Physica, 70 225 (1973).

30 R.J. Munn, F.J. Smith, E.A. Mason and L. Monchick, J. Chem. Phys. 42 537 (1965).

31 S. Imam-Rahajoe, C.F. Curtiss and R.B. Bernstein Jr., J. Chem. Phys. 42 531 (1965).

CHAPTER 3

EXPERIMENTAL DETERMINATION OF DIFFUSION COEFFICIENTS.

3.1 *INTRODUCTION*

The diffusion coefficients reported in this work have been measured at pressures between 1 and 10 atmospheres. The cells in which the measurements have been made are described in the next chapter. It is the intention here to describe the method common to all cells in this laboratory for the precise determination of diffusion coefficients in binary gas mixtures, namely the monitoring with time of the composition of the diffusing system with a matched pair of thermistors forming part of a Wheatstone bridge circuit. In all the cells diffusion takes place vertically along the direction of the axis of a cylindrical channel sealed at each end by a flat end-plate. The thermistors are mounted inside the cell at two points symmetrically disposed about the horizontal plane bisecting the cell. The method is completely analogous to Harned's for the conductimetric measurement of *restricted* diffusion in electrolyte solutions[1]. By Onsager's choice of positions for the two electrodes, the mathematics of the analysis is considerably simplified[21]. Gover[2] applied the same principle to the determination of diffusion coefficients in gaseous mixtures using the relatively crude technique of withdrawing samples simultaneously from the cell through rubber septa located

in the corresponding two positions and injecting the samples into a gas chromatograph for analysis.

The advantage of using thermistors is that gas does not have to be removed from the system for analysis. They respond quickly to changes in concentration by virtue of their sensitivity to the thermal conductivity of their surroundings. The use of thermistors in monitoring diffusion is not new[3,4] but more recently, workers using improved techniques have been able to claim a precision in $\mathcal{D}_{12}$ of 0.2% or better[5-13]. Experimental evidence will be given later in this chapter that difference in resistance of two thermistors in a cell is essentially proportional to the difference in composition of the gas mixture at the monitoring positions. It will be shown that the diffusion coefficient can be calculated from the following equation by the method of least squares:

$$F(t) \equiv \Delta R(t)-\Delta R(\infty) = A'\exp(-\pi^2\mathcal{D}_{12}t/L^2), \qquad (3.1)$$

where A' is a constant, L is the length of the cell, and $\Delta R(\infty)$ is the difference in resistance between the two thermistors at equilibrium. This quantity is non-zero because the thermistors are not perfectly matched.

Since the diffusion coefficient is sensitive to temperature and pressure it is essential that the diffusion apparatus be thermostatted and be impregnable to leaks. In addition these quantities must be measured accurately to enable the absolute determination of $\mathcal{D}_{12}$. A short description of the apparatuses for controlling the temperature and measuring the pressure will be given at the

conclusion of the chapter.

3.2 *THE USE OF THERMISTORS TO MONITOR DIFFUSION*

A thermistor is a semiconductor device whose resistance is very sensitive to temperature. Since the heat generated by a current passing through a thermistor may be sufficient to change its resistance markedly, the "true" resistance can only be measured at very low power. Under these conditions the temperature dependence is governed by the relation[14]

$$R_2 = R_1 \exp[\beta(1/T_2 - 1/T_1)] \qquad (3.2)$$

where R_i is the resistance of the thermistor at absolute temperature T_i, and β is a constant related to the material of the thermistor. Eq. (3.1) is the integrated form of the equation defining the temperature coefficient of resistance, α for a thermistor:-

$$\alpha = (1/R)(dR/dT) = -\beta/T \ . \qquad (3.3)$$

The thermistor material is a mixture of metallic oxides. Its temperature coefficient is large and negative, a typical value of α being about -4% per degree, in contrast to a small positive value for most metals, for example +0.4% per degree for platinum.

It is the "self-heating" effect of thermistors which makes them highly suitable for monitoring changes in environmental conditions. When sufficient current passes through the thermistor to raise its temperature above the ambient value, its resistance falls, thereby permitting more current to pass and heating the thermistor further. Unless

the current is limited by putting a suitable resistor in series, the thermistor may be destroyed. The thermistor eventually assumes a final resistance corresponding to its steady state temperature. This resistance will depend upon the rate at which the heat generated in the thermistor is dissipated. The thermal conductivity of the surrounding gas will influence this to a large extent. The other mechanisms for the heat dissipation may be controlled by suitable design of the thermistor assembly. Convection is minimised by making the thermistor as small as possible and conduction by the leads is kept to a minimum by making them as fine as practicable. Since different gases generally have different thermal conductivities they can be discriminated in principle by measuring the resistance of the thermistor in each gas. Where thermistors are used for analysing the composition of gas mixtures the method works best when the component gases have widely differing thermal conductivities. For example the thermal conductivity of helium is nearly an order of magnitude greater than that of argon.

In this application the composition of the gas mixture is not determined directly, but the difference in resistance between two *matched* thermistors, mounted at positions L/6 and 5L/6 in a cell of length L, is monitored at known time intervals using a Wheatstone bridge circuit. Until recently it had been *assumed* that the difference in resistance between the two thermistors was directly proportional to the difference in composition at the monitoring positions[5]. This assumption has since been justified analytically for

the particular bridge circuit used in conjunction with a digital voltmeter[15,16] but not with the "nulling" circuit used originally[5]. An experimental verification of the proportionality using the helium-argon as a test system is presented in the next section.

The thermistors used in this work were type G112P, supplied in matched pairs by Fenwal Electronics, Inc. (Framingham, Massachusetts). Each unit consisted of a small bead of "type B" material about 0.36mm in diameter coated with glass for protection from oxidation. The leads were made from platinum-iridium wire 0.025 mm in diameter, and were soldered to a bracket mounted on a glass hermetic seal. The thermistor material had a β value of about 3500 K and was selected so that each pair was matched in helium to within about 0.7% of the nominal value of 8000 ohms at 298.16 K.

3.3 *EVIDENCE FOR THE PROPORTIONALITY BETWEEN RESISTANCE AND COMPOSITION DIFFERENCES*

The proportionality assumption mentioned above was tested by a simple experiment which simulated a normal diffusion experiment by "taking snapshots", as it were, of successive stages in the run. This technique was accomplished in the separate compartments of a Loschmidt-type cell[17]. The compartments were of equal volume and the contents were made up to the same pressure with the aid of a Bourdon gauge (Texas Instruments, Houston). Helium-argon gas mixtures were prepared *in situ* by partial pressures in such a way that the mole fraction of helium in the top compartment was always equal to the mole fraction of argon in the bottom

compartment, the lighter mixture always being in the top. In this way, the measurement of a series of resistance differences over a range of mole fraction differences from 1.0 to 0.0, simulated an actual diffusion experiment in which pure helium diffused into pure argon by the lining up of the two compartments.

The results are summarised in Table 3.1. All the mole fractions x refer to argon, with compositions in top and bottom compartments being distinguished by superscripts T and B respectively.

TABLE 3.1

Resistance of thermistors versus composition of He/Ar

x^T	x^B	Δx	$\Delta R(\Omega)$	$\Delta R'(\Omega)$
0.0000	1.0000	1.0000	1320.46	1321.59
0.1250	0.8749	0.7499	963.20	964.33
0.2499	0.7501	0.5002	619.06	620.19
0.3750	0.6250	0.2500	304.77	305.90
0.4200	0.5801	0.1601	191.63	192.76
0.4599	0.5400	0.0799	100.81	101.94
0.5000	0.5000	0.0000	-1.13	0.00

The quantity $\Delta R'$ was obtained by subtracting the last ΔR value in the table from the rest. This particular value, obtained when the concentrations in the top and bottom compartments were equal, is analogous to the equilibrium value, $\Delta R(\infty)$, obtained in a real experiment (See Eq. (3.1)). In both cases, the non-perfect matching of the thermistors

accounted for small residual values of ΔR.

The variation in $\Delta R'$ versus Δx over the range $0 \leqslant \Delta x \leqslant 1$ could best be represented by the equation

$$\Delta R' = 3._1 + 1160\Delta x + 160(\Delta x)^2 \qquad (3.4)$$

for which a maximum deviation of 9 ohms could be expected at the 95% confidence level.

In a real diffusion experiment, only the range $0 < \Delta x < 0.1$ would normally be measured, corresponding roughly to a maximum resistance difference of 100 ohms. The variation of the slope of the curve (3.4) over this range is only about 2%, thus there is no serious error made in assuming that the difference in resistance of the two thermistors in the cell is directly proportional to the difference in gas composition at the two monitoring positions, that is, if K is a constant,

$$\Delta R(t) - \Delta R(\infty) = K\Delta x. \qquad (3.5)$$

3.4 *MEASUREMENT OF ΔR DURING DIFFUSION*

The bridge circuit used for monitoring concentration changes during diffusion is shown in Fig. 3.1. It consisted of the pair of matched thermistors with resistances denoted by R_{31} (top thermistor) and R_{21} (bottom thermistor) and two mica-card standard resistors R_{43} and R_{42} with resistances specified to be within 0.05% of 5000 ohms. The bridge served as a divider to a constant voltage supply, V. A digital voltmeter interfaced to a scanning device measured the voltages V_{32} and V_{42} in rapid succession and these values were recorded automatically on paper tape by a data-logging

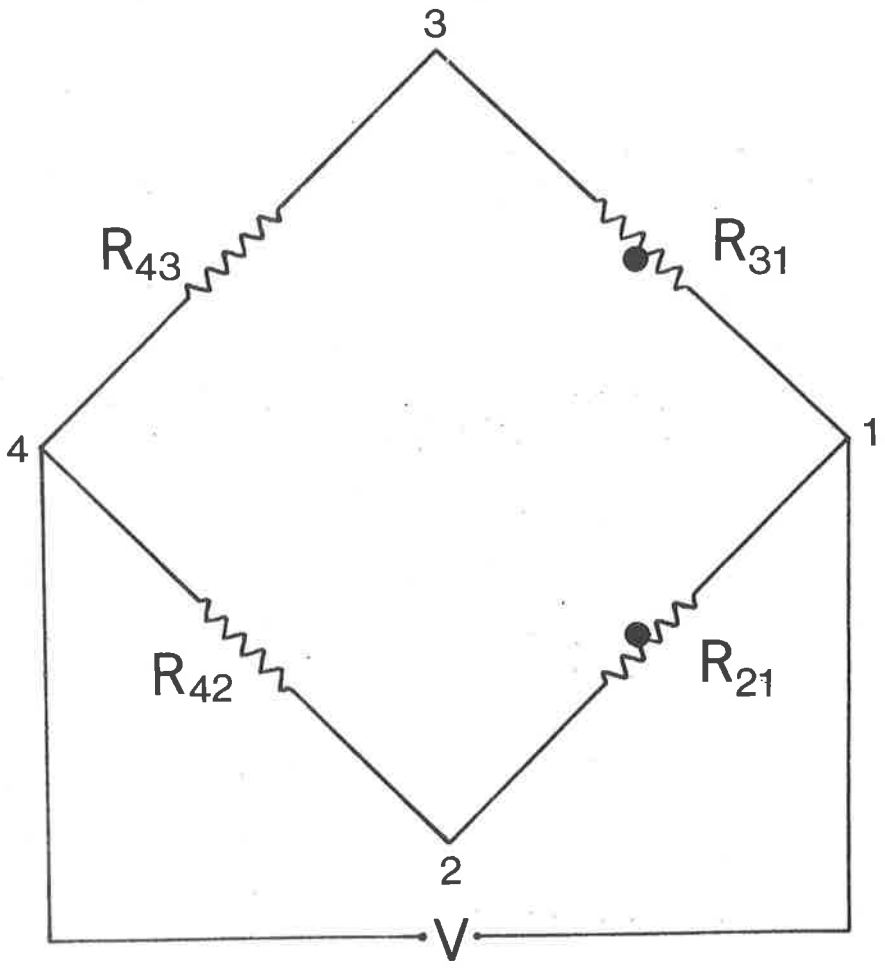

Fig. 3.1: The Wheatstone bridge circuit used for monitoring concentration changes due to diffusion.

device (Schlumberger, U.K.). The difference in resistance between the two thermistors was calculated from

$$\Delta R = (R_{31}-R_{21}) = (R_{42}/V_{42})V_{32}V/(V_{42}-V_{32}) \qquad (3.6)$$

where V was the output from the power supply (usually 3.500 volts). The above equation is exact if the resistances R_{43} and R_{42} are identical.

It is believed that the operation of this bridge is more correct than that originally used in which ΔR was equal to the resistance on a decade box required to "null" the bridge[5]. Yabsley and Dunlop[15] have shown that it is not possible to obtain the correct diffusion coefficient with the original method because the power dissipated by the thermistors depends not only on the change in composition of the surrounding gas, but also to a large extent on the process of "nulling" the bridge.

Although the two voltages on the present bridge were not sampled simultaneously (due to the approximate recording time of 0.32 seconds on the tape punch) this did not present a significant source of error because the following voltage, V_{42}, varied much more slowly than the leading voltage, V_{32}.

At the commencement of the diffusion process, sampling was withheld until V_{32} had fallen to about 20 millivolts, corresponding to a ΔR value of about 100 ohms. From that point, between 100 and 150 readings were taken at equal time intervals which had been preset on an electronic timing device. The intervals were chosen so that an optimum portion of the resistance-versus-time curve was sampled. A further 20 readings were taken after the system had reached

equilibrium.

3.5 *CALCULATION OF THE DIFFUSION COEFFICIENT*

In order to calculate the diffusion coefficient, the way in which the composition of the gas mixture changes with time must be known. The diffusion process is governed by Fick's second law, which, for one-dimensional diffusion in a binary mixture, is approximated by Eq. (2.9). For convenience it is repeated here:-

$$(\partial c_i/\partial t)_{z,T,P} = \mathcal{D}_{12}(\partial^2 c_i/\partial z^2)_{t,T,P} \qquad (3.7)$$

where $c_i(z,t)$ is the concentration of the i^{th} species at time t, at position z along the direction of diffusion at constant temperature and pressure.

To solve Eq. (3.7) uniquely for $c_i(z,t)$ under the experimental conditions, the appropriate boundary and initial conditions must be specified. Since the diffusion is taking place inside a closed vessel it is termed *restricted* diffusion. The gas cannot diffuse past the end plates, so the *boundary* conditions may be stated as:

$$\partial c_i(0,t)/\partial z = \partial c_i(L,t)/\partial z \equiv 0 \qquad (3.8)$$

where L is the length of the cell. We shall let $z = 0$ at the top of the cell and $z = L$ at the bottom. Furthermore, we shall drop the subscript i from $c_i(z,t)$ but understand that the concentration of the *heavier* component in the mixture is being referred to. The general solution of Eq. (3.7) subject to the conditions (3.8) is[18]

$$c(z,t) = B_0 + \sum_{k=1}^{\infty} B_k \exp(-k^2\pi^2\mathcal{D}_{12}t/L^2)\cos(k\pi z/L) \qquad (3.9)$$

which, at zero time, reduces to the cosine Fourier series,

$$c(z,0) = B_0 + \sum_{k=1}^{\infty} B_k \cos(k\pi z/L). \qquad (3.10)$$

The Fourier coefficients depend on the form of the initial concentration distribution. In this laboratory, the initial distribution is approximately a step function:

$$c(z,0) = c(0,0) + u(z-\alpha)c(L,0) \qquad (3.11)$$

where

$$u(\xi) = \begin{cases} 0, & \xi \leq 0 \\ 1, & \xi > 0 \end{cases} \qquad (3.12)$$

and α ($0 \leq \alpha \leq L$) is the position of the "jump" or "boundary" in the cell. By equating the initial concentration distribution to the Fourier series (3.10) and evaluating the coefficients (see Appendix C), the concentration distribution function is uniquely determined.

The symmetry properties of the solution (3.9) enable considerable simplification to be made[1]. If the concentration is measured at positions z and L-z in the cell, all terms involving even values of k, including k=0, vanish when the difference $\Delta c(t)$ is taken. Furthermore, if z is chosen to be L/6, additional terms vanish when k is a multiple of 3. The solution can now be written

$$\Delta c(t) = A_1 \exp(-\pi^2 \mathcal{D}_{12} t/L^2) - A_5 \exp(-25\pi^2 \mathcal{D}_{12} t/L^2) + \ldots \qquad (3.13)$$

where $A_k = -\sqrt{3}B_k$ (B_k is defined in Appendix C).
The second term in Eq. (3.13) very rapidly becomes negligible compared with the first by virtue of the factor 25 in the exponent. In principle, therefore, one can calculate the diffusion coefficient $\mathcal{D}_{12}$, by fitting a set

of measured concentration differences as a function of time to an equation of the form

$$y(t) = A \exp(-t/\tau), \tag{3.14}$$

where τ is the relaxation time of the system given by

$$\tau = L^2/\pi^2\mathcal{D}_{12}, \tag{3.15}$$

Now since we have shown that $\Delta R(t)-\Delta R(\infty)$ is directly proportional to Δx, and since for gases in a fixed volume, Δx is proportional to Δc, we may use the equation

$$\Delta R(t)-\Delta R(\infty) = A' \exp(-t/\tau) \tag{3.16}$$

to determine $\mathcal{D}_{12}$ by the method of non-linear least-squares[19]. Since $\mathcal{D}_{12}$ varies approximately inversely with pressure it is convenient for comparison purposes to calculate the more slowly-varying product $p\mathcal{D}_{12}$ which is numerically equal to the value of $\mathcal{D}_{12}$ "corrected" to 1 atmosphere pressure if p is expressed in atmospheres.

In this work the reliability of the data could be tested by fitting the set of resistances $\Delta R(t)$ to equation (3.16) in which $\Delta R(\infty)$ was an extra parameter to be determined. An experiment was considered to be "good" if the experimental and calculated values of $\Delta R(\infty)$ were in concordance to within 0.02 ohms. To eliminate the possibility of such agreement being merely fortuitous, successive groups of data points were left out from the beginning of the set and $\Delta R(\infty)$ was recalculated. In this respect a set of self-consistent values of the calculated $\Delta R(\infty)$ could be considered to be a stronger criterion for a "good" run. The uncertainty in $\mathcal{D}_{12}$ was usually well within 0.1%.

3.6 *MEASUREMENT OF PRESSURE*

The introduction of gases into the cell and their removal was accomplished with the aid of a manifold which linked the cell to the gas cylinders, the vacuum system and a Bourdon pressure gauge. The vacuum system consisted of a large T-shaped manifold providing "vacuum on tap" to two independent diffusion apparatuses. The base of the "T" was connected through a bypass system to a rotary pump and a water-cooled silicone oil diffusion pump.

The pressure transducer in the Bourdon gauge consisted of a hollow quartz spiral with a small mirror at the end housed in a capsule with two outlets. One outlet connected the spiral to the system under test and the other connected the rest of the capsule to the vacuum system. In this mode absolute pressures could be determined on the gauge by measuring the degree of unwinding of the spiral due to the pressure difference across its walls. The rotation of the spiral was registered on a decade counter via a photocell detector linked with a servo motor. This reading could be converted into units of pressure by interpolating from a calibration chart supplied by the manufacturer. In this work a capsule suitable for operation up to 14 atmospheres was used. A least squares analysis of the calibration data showed that the pressure p in torr could be calculated to within ±0.02% from the gauge reading, G, using the formula

$$p = 51.7149\, G\,(0.565_4 + 0.00002_5\, G). \qquad (3.17)$$

3.7 *TEMPERATURE CONTROL*

The diffusion cell was completely immersed in a bath

of deionized water kept constantly stirred with a rotor powered by a $^{1}/3$ h.p. electric motor. In all experiments the water temperature was maintained to within ±0.001 of 300K as measured on a mercury-in-glass thermometer (Dobros, Australia) which had been calibrated against a platinum resistance thermometer. Constant temperature was achieved with a mercury-toluene relay[20] connected to a 12 ohm pyrotenax element mounted in the bath. The heat output of the element was controlled by a thyratron regulator. For the temperature control to be effective, the room temperature was kept below that of the bath so that the water would always be tending to cool. Since the bath had a large capacity (about 625 litres), the controller alone usually could not compensate for heat losses. This was partially overcome by using a base heater consisting of a 35 ohm pyrotenax element through which the current from a variable A.C. voltage source was passed. Heat loss through the glass at the front of the bath was minimised by mounting a moulded polystyrene foam board against it on the outside.

REFERENCES

1 H.S. Harned and D.M. French, Ann. N.Y. Acad. Sci., 46 267 (1945).

2 T.A. Gover, J. Chem. Educ., 44 409 (1967).

3 R.R.J. van Heijningen, A. Feberwee, A. van Oosten and J.J.M. Beenakker, Physica, 32 1649 (1966).

4 R.R.J. van Heijningen, J.P. Harpe and J.J.M. Beenakker, Physica, 38 1 (1968).

5 P.J. Carson, P.J. Dunlop and T.N. Bell, J. Chem. Phys. 56 531 (1972).

6 M.A. Yabsley and P.J. Dunlop, Phys. Letters, 38A 247 (1972).

7 K.R. Harris, T.N. Bell and P.J. Dunlop, Can. J. Chem. 50 1874 (1972).

8 K.R. Harris, T.N. Bell and P.J. Dunlop, Can. J. Phys. 50 1644 (1972).

9 P.J. Carson and P.J. Dunlop, Chem. Phys. Letters, 14 377 (1972).

10 P.J. Carson, M.A. Yabsley and P.J. Dunlop, ibid. 15 436 (1972).

11 G.R. Staker, M.A. Yabsley, J.M. Symons and P.J. Dunlop, J. Chem. Soc., Faraday Trans. I, 70 825 (1974).

12 K.R. Harris and T.N. Bell, Can. J. Phys. 51 2101 (1973).

13 G.R. Staker, P.J. Dunlop, K.R. Harris and T.N. Bell, Chem. Phys. Letters, 32 561 (1975).

14 Fenwal Electronics, Framingham, Massachusetts, "Thermistor manual".

15 M.A. Yabsley and P.J. Dunlop, J. Phys. E: Sci. Instr. 8 834 (1975).

16 M.A. Yabsley, Ph.D. thesis, University of Adelaide (1975).

17 J. Loschmidt, Sitzber. Akad. Wiss. Wein, 61 367 (1870).

18 H.S. Carslaw and J.C. Jaeger, "Conduction of heat in solids", Oxford University Press (1947).

19 J.R. Wolberg, "Prediction analysis", Van Nostrand (1967).

20 R.H. Stokes, N.Z. J. Sci. Technol. B, 27 75 (1945).

CHAPTER 4

THE DIFFUSION CELLS

4.1 *INTRODUCTION*

Although high *precision* in the determination of $\mathscr{D}_{12}$ for gas mixtures has been claimed in this laboratory[1,2] it has been found that there are some discrepancies when cells of different types and different sizes are used. In this study, two types of cell using matched thermistors to monitor diffusion were compared. Three cells of each type had been constructed, each differing in some aspect of their geometry. To facilitate the discussion somewhat, those of the first type have been labelled A1, A2 and A3, and those of the second type have been labelled B1, B2 and B3.

The original form of the first type of cell, type A, has been described in detail by Carson and co-workers[1]. The type B cell, based on the design of Loschmidt[3,4] has been described by Staker et al.[2]. A comparison of all six cells was made by measuring in each, the composition dependence of diffusion in the *helium-nitrogen* system at 300K and a pressure of 1 atmosphere. The results of the investigation showed that only in category B did the results for the three cells agree within the estimated experimental precision of 0.2% over the whole composition range. Furthermore, results for the argon-nitrogen system in the type B cells were in complete agreement with experiments

analysed with a mass spectrometer[5]. In the light of these findings a more detailed discussion of the comparative features and operations of the cells is given below. In particular, a description is given of a new cell which was used subsequently in the pressure dependence study of diffusion.

The results for helium-nitrogen are compared with the predictions of the Chapman-Enskog theory.

4.2 *A-TYPE CELLS - DESCRIPTION*

Each cell in this category consisted of a closed cylindrical vessel with a vertical jet screwed into each end plate, the outlets being made flush with the inner surfaces.

The passage of gas through each jet was controlled by a bellows valve (Nupro Co., Cleveland, Ohio), mounted in close proximity to each jet on the outside. Various other types of jets have been tested[6], namely those which protrude into the cell and direct the gas horizontally instead of vertically into the cell. These jets, however, were not used in this investigation. An illustrated description of a representative A-type cell (A1) has been given elsewhere[1]. The precise internal lengths of the three cells and the internal diameters are listed in Table 4.1.

TABLE 4.1

Dimensions of the A-type cells

Cell	Length (cm.)	Internal diam. (cm.)
A1	102.00	4.65
A2	45.019	4.65
A3	44.999	2.45

Cells A1 and A2 were constructed from type 316 stock stainless steel tubing (wall thickness 0.16 cm.), whereas A3 was machined from a block of brass 7.6 cm. in diameter.

4.3 *A-TYPE CELLS - EXPERIMENTAL METHOD*

With the aid of a manifold and the Bourdon pressure gauge the first gas was introduced into the cell until its pressure was between 90 and 95% of the *final* pressure. Generally, the first gas was a mixture prepared *in situ* by partial pressures. The cell was isolated from the manifold by closing the bellows valves and the gas inside was allowed to come to thermal equilibrium and to mix completely, if applicable. When the difference in resistances of the thermistors had become constant,the second gas was carefully introduced at the top or the bottom, depending on its density relative to the first gas, until the required final pressure was obtained. The cell was then isolated before the diffusion process was monitored.

It was *assumed* in this method that the initial turbulence that must inevitably have been set up when the second gas was added, disappeared by the time readings were taken.

4.4 *B-TYPE CELLS - DESCRIPTION*

Two of the B-type cells,designed basically after Loschmidt[3] and Strehlow[4], consisted of two identical cylindrical compartments mounted on opposite sides of a pair of stainless steel circular plates 18 cm. in diameter, clamped together about a common pivot by a set of coil springs. The sliding surfaces of the plates were lapped

optically flat and separated by a thin layer of Apiezon T-grease to provide the best possible vacuum seal and the minimum hindrance to rotation. The cell B1 has been described in more detail elsewhere[2].

B2 was very similar to B1 but was designed primarily for diffusion runs above atmospheric pressure. Heavier duty springs were used to reduce the likelihood of gas escaping from the cell between the plates. As a further safeguard, two viton O-rings were inserted between the plates into two circular grooves concentric with the pivot. One groove was close to the pivot and the other was close to the outside edge of the plates.

A third cell B3, which was radically different in construction to the first two, is shown in Fig. 4.1. It was machined from a cylindrical brass block 18.73 cm. in diameter. *Two* diffusion channels, 180° apart were honed out parallel to the axis of the block. The block was then cut exactly in half, perpendicular to the axis, and the two adjacent surfaces,I,were lapped optically flat. As with the other B-type cells,the sliding surfaces were lubricated by a thin layer of T-grease as one block rotated with respect to the other about a central stainless steel pivot, R, which was 1.90 cm. in diameter. The two halves of the brass block were held firmly together by an assembly of cupped washers,S, which, when compressed a total distance of 1 mm. by the stainless steel nuts, N, exerted a restoring force of 27 kN on the ends of the blocks. Forces of this order of magnitude were necessary to prevent gas from escaping through the greased interface at high pressures

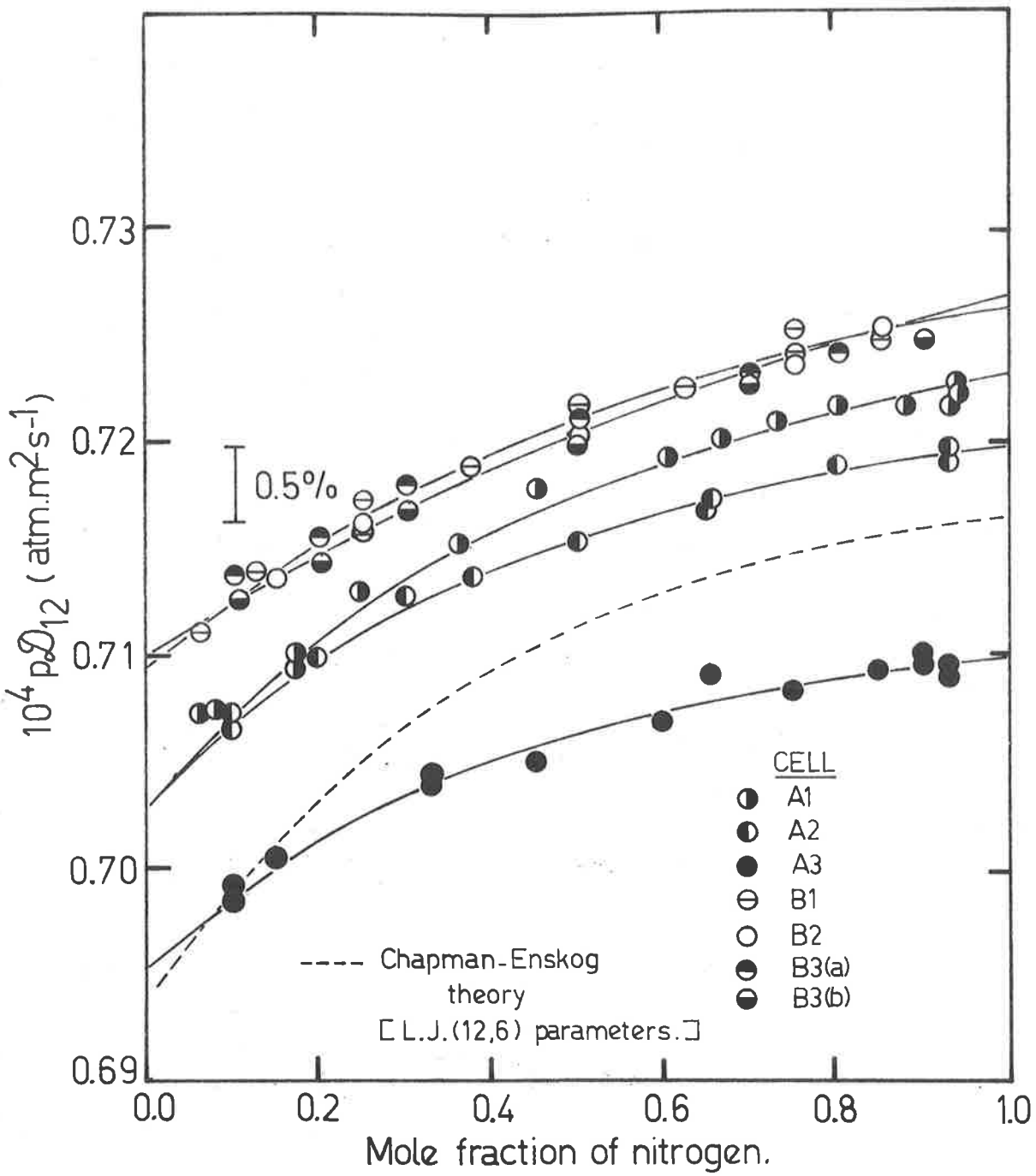

Fig. 4.2: The composition dependence of the binary diffusion coefficient for helium-nitrogen at 300K and 1 atm. pressure in different cells.

(about 10 atmospheres). In this respect,this cell was an improvement on B2 which failed to hold pressure satisfactorily above 3 atmospheres. There were four separate compartments in the brass Loschmidt cell which, when lined up, formed two independent diffusion columns which we shall denote by B3(a) and B3(b).

The lengths and internal diameters of the B-type cells are summarised in Table 4.2.

TABLE 4.2

Dimensions of the B-type cells

Cell	Length (cm.)	Internal diam. (cm.)
B1	117.34	4.65
B2	45.038	4.65
B3(a)	40.049	2.54
B3(b)	40.049	3.81

4.5 *B-TYPE CELLS - EXPERIMENTAL METHOD*

Isobaric gas mixtures were prepared *in situ* in the separate compartments by the method of partial pressures. Each compartment was then isolated from the manifold by closing the bellows valves and the mixtures were allowed to equilibrate. The usual practice in a B-type cell was to make up a mixture in one compartment only,and to have a pure gas in the other compartment. In cell B3, this of course, could be done in duplicate with the four compartments. At the commencement of a run,the compartments were brought into alignment, thereby creating an initial

concentration distribution closely approximating that of a step function with the "jump" (the boundary) at z = L/2 (c.f. Eq. (3.11)).

4.6 *FEATURES IN COMMON*

In all cells the concentration changes were monitored by a pair of matched thermistors mounted symmetrically at a distance L/6 from each end and connected by shielded cables to the opposite arms of a Wheatstone bridge (Fig. 3.1) to which was applied a constant potential difference of 3.500 volts. Viton O-rings were incorporated in the thermistor mounting assembly to prevent unwanted leaks at these points. All other non-moving metal-metal surface contacts were sealed by lead O-rings, A (Fig. 4.1), prepared *in situ* by moulding lead wire into circular V-shaped grooves. This particular feature was incorporated in the construction of the cells except A1 and A2 in which Viton O-rings were used exclusively.

Each cell, when in use, was mounted in the water bath on an adjustable three-point suspension and was levelled prior to first usage to ensure that diffusion column was truly vertical. All operations involving the introduction, removal and measurement of the pressure of the gases in the cell were carried out with the aid of a manifold consisting of a framework of rigid and flexible stainless steel tubing and a number of bellows valves. The "plumbing" was made pressure-tight at the joints by using Swagelok double-ferrule fittings (Crawford Fittings, Cleveland, Ohio).

4.7 *THE COMPOSITION DEPENDENCE OF $\mathcal{D}_{12}$ FOR HELIUM/NITROGEN*

In each cell, a series of diffusion experiments at 300K and a pressure of 1 atmosphere was carried out as a function of composition in helium-nitrogen mixtures. The results for each cell are listed in Table 4.4. The quantities in each column are, respectively, the mole fraction of nitrogen, $x(N_2)$, the pressure p in atmospheres and the product $p\mathcal{D}_{12}$, which is numerically equal to the effective value of the mutual diffusion coefficient at one atmosphere pressure. An equation most suitable for representing the concentration dependence data is[7,8],

$$p\mathcal{D}_{12} = a + bx_2/(1+cx_2) \qquad (4.1)$$

where x_2 is the mole fraction of nitrogen, and a, b and c are constants. The constants could be obtained by fitting Eq. (4.1) to the composition dependence data by a non-linear least-squares procedure[9]. A summary of the least-squares analysis is given in Table 4.3. The quoted uncertainties in the coefficients represent the error limits at the 95% confidence level.

TABLE 4.3

Least-squares results for He/N_2 using Eq. (4.1)

Cell	*ax10^4	b	c	*Std.dev.x10^8
A1	0.7048 ± 0.0017	0.043 ± 0.018	1.37 ± 0.40	8.1
A2	0.7028 ± 0.0013	0.048 ± 0.014	1.82 ± 0.63	3.4
A3	0.6952 ± 0.0022	0.062 ± 0.033	1.9 ± 1.2	5.8
B1	0.7110 ± 0.0038	0.027 ± 0.025	0.56 ± 1.3	3.2
B2	0.7091 ± 0.0018	0.039 ± 0.017	1.25 ± 0.88	6.2
B3(a)	0.7106 ± 0.0016	0.033 ± 0.013	1.16 ± 0.77	2.7
B3(b)	0.7099 ± 0.0014	0.027 ± 0.010	0.72 ± 0.58	2.4

*Units are atm.m^2.s^{-1}

TABLE 4.4

Diffusion data for He/N_2 at 300K

$x(N_2)$	p/atm.	$10^4 p\mathfrak{D}_{12}$/atm.$m^2 s^{-1}$
	Cell A1	
0.061_8	1.000_0	0.707_2
0.078_2	1.002_5	0.710_1
0.079_3	0.999_8	0.707_4
0.080_0	1.000_0	0.707_2
0.171_7	1.008_6	0.709_4
0.172_6	1.009_4	0.710_1
0.248_3	1.003_6	0.713_0
0.362_4	1.010_0	0.715_3
0.453_7	1.010_9	0.717_7
0.605_7	1.009_0	0.719_4
0.666_8	1.007_5	0.720_1
0.669_8	1.010_5	0.719_1
0.734_4	1.002_0	0.720_0
0.747_1	1.013_2	0.720_9
0.802_4	1.010_5	0.721_6
0.879_9	0.992_1	0.721_7
0.919_8	1.000_2	0.722_7
0.937_9	0.980_8	0.722_5
0.939_5	0.979_3	0.721_7
0.939_8	0.979_8	0.722_2
	Cell A2	
0.098_9	0.998_7	0.707_2
0.100_1	1.000_2	0.706_6
0.199_9	0.999_9	0.709_6
0.299_7	0.999_7	0.712_7
0.376_8	0.999_7	0.713_6
0.377_1	1.000_5	0.713_6
0.500_0	1.000_1	0.715_3
0.650_3	0.999_8	0.716_9
0.653_0	1.000_2	0.717_3
0.800_0	1.000_1	0.718_9
0.930_0	0.999_8	0.719_8
0.930_1	0.999_9	0.719_7
0.930_2	0.999_8	0.719_0

cont.

TABLE 4.4 (cont'd.)

$x(N_2)$	p/atm.	$10^4 p\mathcal{D}_{12}$/atm.m^{2}s^{-1}
	Cell A3	
0.100_0	1.000_0	0.698_3
0.100_3	1.000_3	0.699_2
0.149_7	0.999_8	0.700_5
0.329_9	0.999_9	0.704_3
0.330_0	1.000_0	0.703_9
0.334_1	1.000_0	0.703_9
0.449_8	0.999_7	0.704_9
0.600_3	1.088_7	0.706_8
0.653_6	1.000_0	0.709_1
0.750_1	1.000_0	0.708_4
0.850_0	1.000_0	0.709_2
0.899_9	1.000_2	0.710_1
0.900_1	0.999_9	0.709_5
0.929_9	0.999_9	0.709_6
0.930_1	1.000_4	0.709_0
	Cell B1	
0.150_0	0.880_8	0.713_5
0.250_0	0.880_8	0.716_1
0.500_0	0.880_8	0.720_3
0.750_0	0.880_8	0.723_8
0.850_0	0.880_8	0.725_5
	Cell B2	
0.062_5	1.000_1	0.711_0
0.125_0	1.000_0	0.713_9
0.249_9	1.000_3	0.715_9
0.250_0	1.000_0	0.717_2
0.374_9	1.000_0	0.718_8
0.500_0	1.000_0	0.721_7
0.500_0	1.000_1	0.721_6
0.500_0	1.000_2	0.721_1
0.500_0	1.000_1	0.720_2
0.500_0	1.000_5	0.720_8
0.625_0	1.000_0	0.722_5
0.749_9	1.000_2	0.725_2
0.750_0	1.000_0	0.724_0
0.850_0	1.000_0	0.724_8

cont.

TABLE 4.4 (cont'd.)

$x(N_2)$	p/atm.	$10^4 p\mathcal{D}_{12}$/atm.m^{2}s^{-1}
	Cell B3(a) (diam. = 2.54 cm.)	
0.100_1	1.000_0	0.713_7
0.200_2	1.000_0	0.715_5
0.300_1	1.000_4	0.717_9
0.500_0	1.000_0	0.721_2
0.699_9	1.000_1	0.723_1
0.799_9	1.000_3	0.724_2
0.899_8	1.000_2	0.724_9
	Cell B3(b) (diam. = 3.81 cm.)	
0.100_1	1.000_4	0.712_6
0.200_1	1.000_2	0.714_3
0.299_9	1.000_1	0.716_6
0.500_2	1.000_0	0.720_0
0.700_0	1.000_1	0.722_5
0.900_0	1.000_0	0.724_6

The data in Table 4.4 and the curves obtained from Table 4.3 are plotted in Fig. 4.2.

4.8 *DISCUSSION*

An examination of Fig. 4.2 readily shows that there is a considerable variation in the diffusion data between different cells. It may be observed however, that the major variation occurs between type A cells, the fixed-section type. For example, when cells of different lengths but with the same internal diameter are compared (A1 and A2) it is seen that the values of $p\mathcal{D}_{12}$ are in reasonable agreement at the helium-rich end of the mole fraction scale, but differ by about 0.4% at the nitrogen-rich end. For the cells with the same length but with different internal diameters (A2 and A3) the composition dependences are very similar but the corresponding values of $p\mathcal{D}_{12}$ differ by about 1.2%!

In marked contrast to the above behaviour, all results obtained in the Loschmidt (B) type cells are consistent to about 0.2%, which is of the order of the experimental error. The curves for cells B3(a) and B3(b) have been omitted from Fig. 4.2 for clarity.

The apparent geometry dependence of the diffusion coefficient in the A-type cells seems to be a consequence of the "squirt-in" technique for setting up an initial concentration distribution. Since this dependence is not exhibited in the Loschmidt cells it must be an artefact and therefore such a technique is the wrong one to use in restricted diffusion cells. An undesirable feature of the A-type cells is the small "dead space" between the jet and the seat of

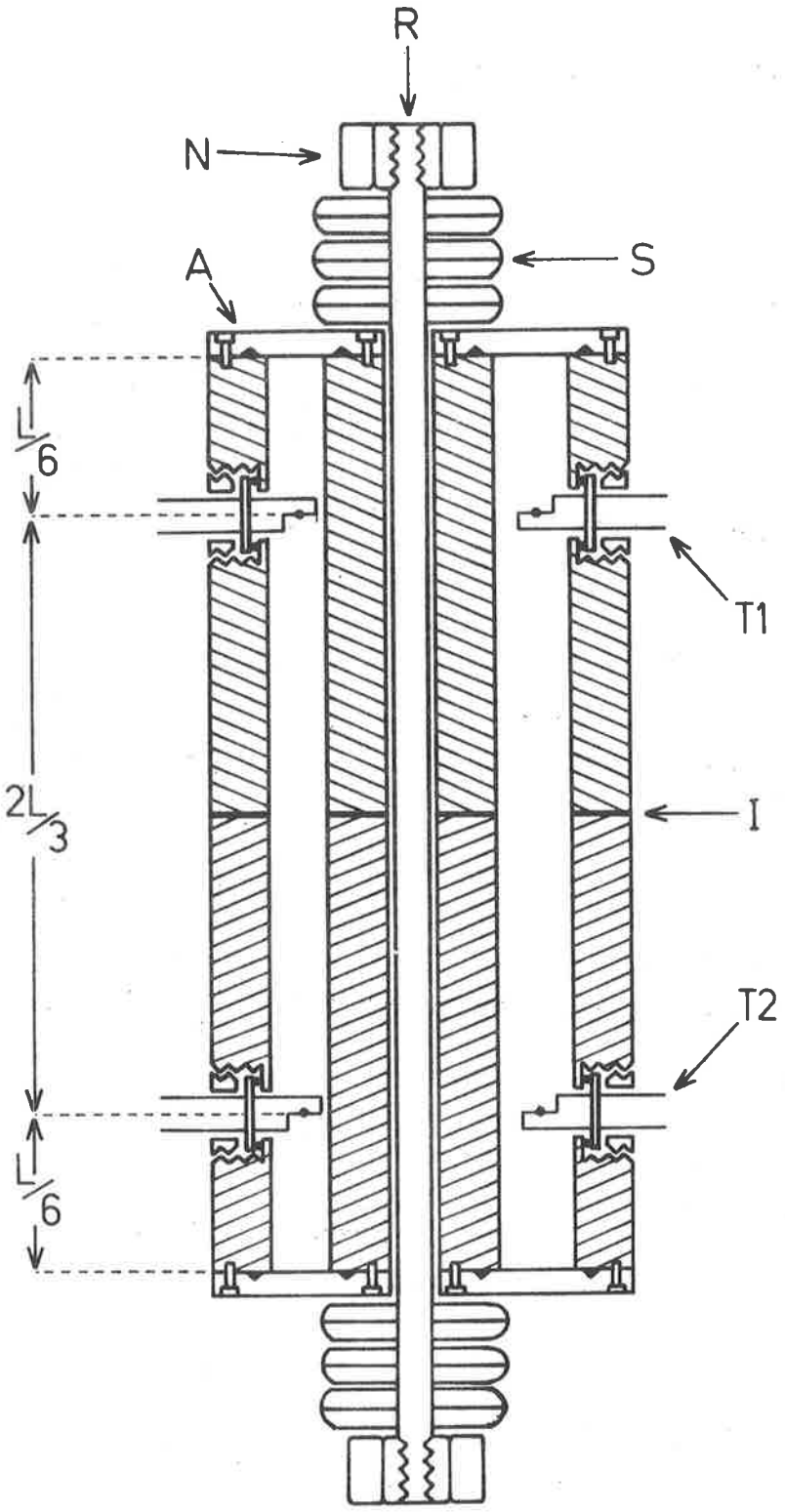

Fig. 4.1: The brass Loschmidt-type cell, B3. T1 and T2 are the top and bottom thermistors respectively. Other symbols are referred to in the text.

the Nupro valve. Since the space cannot be isolated in this type of cell, gas is diffusing through the jet at the same time as the main diffusion process is taking place. One might therefore expect that diffusion coefficients in cell A3 will be affected the most,whereas,in cell A1, which is 8 times as large, this effect will be least pronounced. This is consistent with the trend in Fig. 4.2.

Such an effect is absent in the Loschmidt-type cells because dead spaces are essentially non-existent. It might be argued that the method of boundary formation in a B-type cell is superior to that in the former type because the pressures in the two compartments are the same. Although experiments in such a cell are always done in this way it has been observed that deliberately-created pressure differences of up to 30% between the compartments prior to diffusion have no effect on the reliability of the run, nor on the final result[10].

An asymmetric Loschmidt cell which creates a boundary close to the bottom end of the cell is being tested at the present time[11]. The final mole fraction of the heavier gas when two pure gases mix is 0.08. The purpose of the cell is to test the hypothesis that the diffusion coefficients are independent of the position of the formation of the boundary. Results to date indicate that for the helium-nitrogen system at $x(N_2) = 0.08$ the diffusion coefficient in the new cell is about 0.5% lower than the corresponding values in the other Loschmidt cells. It is interesting to note that the results for this system and for helium-argon are almost identical with measurements made in an A-type

cell of the same internal diameter, incorporating a special type of jet[18]. This jet has a much smaller dead space associated with it. An important feature of its design is a thin baffle, which protrudes about 0.8 mm into the cell. The incoming gas is deflected horizontally by the baffle ensuring that most of it is initially localised at one end of the cell. One can envisage that the concentration profile formed in this fashion bears a closer resemblance to the idealised step function than the one generated by the simple jets used in cells A1, A2 and A3 where the incoming gas is directed vertically into the cell.

Since the problem of a geometry dependence did not arise in the symmetrical Loschmidt-type cells it was considered that they were giving *accurate* and *precise* results for the absolute determination of the diffusion coefficients. It is interesting and indeed encouraging to note that in the nitrogen-argon system in a 50/50 mixture, a comparison of mass spectrometry and thermistor bridge analysis led to identical results in cell B1 which in turn were identical to those obtained in B3(a) and B3(b)[5].

On this basis, the new brass Loschmidt cell B3 was used in the subsequent systematic pressure dependence study of binary gas mixtures containing helium, the main subject matter of Chapter 5.

4.9 *THE THEORETICAL COMPOSITION DEPENDENCE FOR HELIUM-NITROGEN*

Having precisely established the composition dependence of pD_{12} at 300K and 1 atmosphere for helium-nitrogen in the

Loschmidt cells it was considered worthwhile to compare these results with the Chapman-Enskog theory. The theoretical composition dependence was evaluated at the same temperature and pressure using the Kihara second approximation[12] (Eq. (2.21)) to the Chapman-Enskog formula for the mutual diffusion coefficient. Quantum-corrected collision integrals[13] for the Lennard-Jones (12,6) potential model were used in the calculation[14]. The potential parameters σ_{ij} and ε_{ij}/k and their sources are listed in Table 4.5.

TABLE 4.5

The Lennard-Jones (12,6) parameters for the helium-nitrogen system.

	σ_{ij}(nm)	ε_{ij}/k (K)	Ref.	Method
He-He	0.2576	10.22	15	Viscosity
He-N_2	0.3120	36.18	16	Viscosity
N_2-N_2	0.385	47.6	17	Self-diffusion

The theoretical composition dependence is represented in Fig. 4.2 as a broken line. On comparing this curve with the experimental ones it appears that the Chapman-Enskog theory tends to over-estimate the composition dependence of the diffusion coefficient for the helium-nitrogen system. This is borne out by the comparison of the theoretical and experimental ratios of the diffusion coefficients at the two composition extremes as summarised in Table 4.6.

TABLE 4.6

The comparison of the theoretical ratio, $(p\mathcal{D}_{12})_{x_2=1}/(p\mathcal{D}_{12})_{x_2=0}$, with the experimental ratio.

	$(p\mathcal{D}_{12})_{x_2=1}/(p\mathcal{D}_{12})_{x_2=0}$
Theoretical	1.033
A1	1.026
A2	1.024
A3	1.031
B1	1.024
B2	1.024
B3(a)	1.022
B3(b)	1.022

The theoretical curve lies below the curves for the Loschmidt cells by about 1.7%, a difference that cannot be attributed to experimental error alone, since the estimated precision was about 0.2%. This disagreement is understandable considering that nitrogen molecules are non-spherical and therefore are strictly not suitable for representation by a Lennard-Jones model. The parameters themselves are subject to a wide variation due to varying degrees of experimental precision and different temperature ranges over which the parameters are averaged for this particular potential function.

REFERENCES

1 P.J. Carson, P.J. Dunlop and T.N. Bell, J. Chem. Phys., 56 531 (1972).

2 G.R. Staker, M.A. Yabsley, J.M. Symons and P.J. Dunlop, J. Chem. Soc., Faraday Trans. I, 70 825 (1974).

3 J. Loschmidt, Sitzber, Akad. Wiss. Wein, 61 367 (1870).

4 R.A. Strehlow, J. Chem. Phys., 21 2101 (1953).

5 I.R. Shankland and P.J. Dunlop, Chem. Phys. Letters (1976) (in press).

6 P.J. Carson, Ph.D. thesis, University of Adelaide (1974).

7 I. Amdur and T.F. Schatzki, J. Chem. Phys., 29 1 (1958).

8 T.R. Marrero and E.A. Mason, J. Phys. Chem. Ref. Data, 1 3 (1972).

9 J.R. Wolberg, "Prediction analysis", Van Nostrand (1967).

10 I.R. Shankland, personal communication.

11 T.N. Bell, personal communication.

12 E.A. Mason, J. Chem. Phys., 27 75 (1957).

13 R.J. Munn, F.J. Smith, E.A. Mason and L. Monchick, J. Chem. Phys., 42 537 (1965).

14 The author is grateful to Dr. M.A. Yabsley for the use of his computer program.

15 H.L. Johnston and E.R. Grilly, J. Phys. Chem., 46 948 (1942).

16 J. Kestin, Y. Kobayashi and R.T. Wood, Physica, 32 1065 (1965).

17 E.B. Winn, Phys. Rev., 74 698 (1947); 80 1024 (1950).

18 K. Ayogai, unpublished data.

CHAPTER 5

THE PRESSURE DEPENDENCE OF DIFFUSION

5.1 *INTRODUCTION*

It was shown in the previous chapter that of all the *restricted diffusion* cells constructed in this laboratory, only the Loschmidt type cell could be used for the precise absolute determination of the mutual diffusion coefficient over the whole composition range of helium-nitrogen mixtures at 1 atmosphere and 300K without the ambiguity of an apparent geometry dependence. Cell B2 was the prototype Loschmidt cell for measuring diffusion coefficients at pressures above 1 atmosphere. The failure of this cell to hold pressure satisfactorily above 3 atmospheres led to the design of the brass block diffusion cell, B3. In this cell, there could be no possibility of the surfaces of the interface being distorted by the force of the springs. The cupped washers, which replaced the coil springs, enabled much greater forces to be used in preventing the sliding surfaces from being prised apart by the gases at high pressures. The new feature of two independent diffusion channels of different internal diameters (Table 4.2) and with separate filling ports, enabled duplicate experiments to be carried out simultaneously, hence providing a valuable check on the precision of the data.

Before undertaking a systematic pressure dependence

study in several binary gas mixtures, it was considered worthwhile to investigate to what limits the thermistors could be used reliably in diffusion measurements. The conclusion drawn from this study was that only in mixtures containing excess helium would one consistently obtain the most reliable measurements over the pressure range to be studied. On this basis, diffusion coefficients were measured in binary mixtures of helium with six other gases over the pressure range of 1 to 9 atmospheres. In all experiments helium constituted 90% of the final mixture.

The density dependence was determined from the experimental results and was compared with the Thorne extension to Enskog's theoretical dependence based on the rigid-sphere molecular model. The rigid spheres model as such failed to predict the density dependence satisfactorily for all systems. However, following Enskog's approach, a modified form of Thorne's equation, relatable to equation of state data, was tried and found to give good agreement in most cases.

5.2 *INVESTIGATION OF THE COMPOSITION DEPENDENCE ABOVE ATMOSPHERIC PRESSURE*

As in the previous chapter, helium-nitrogen mixtures were again used as the test system. Having successfully determined the composition dependence of the diffusion coefficient of this system at 1 atmosphere and 300K, to better than 0.2% in both channels of cell B3, a similar determination was attempted at higher pressures, as had previously been done in cell A2[1]. This proved to be unsuccessful at 3 and 5 atmospheres, as can be seen in the

first graph in Figure 5.1. The solid curve represents the *smoothed* composition dependence of the product $p\mathcal{D}_{12}$ at 1 atmosphere evaluated from the *combined* results from both channels of the brass block diffusion cell, B3, which were tabulated in Chapter 4. The apparent composition dependence of $p\mathcal{D}_{12}$ measured at 3 and 5 atmospheres was extremely uncertain, especially towards the nitrogen-rich end of the composition range. This generally coincided with a poor agreement between the resistance-versus-time data and Eq. (3.16). When the pair of thermistors from one diffusion channel were interchanged with the pair from the other, a similar deterioration in the reliability of the experiments at 3 atmospheres was observed as the mole fraction of helium in the final mixtures decreased, although this time the agreement between the two channels had improved considerably, as can be seen in the second graph in Figure 5.1. The latter position of the thermistors was retained for the remainder of the project.

It has been suggested[1] that a larger proportion of energy is dissipated from the thermistors by *convection* as the density of the gas increases. It therefore appeared that the best way to study the density dependence of binary diffusion with the minimum interference from the convective effect, was to limit the experiments to mixtures in which helium was in excess. This unfortunately narrowed the scope of the project, in which a pressure-composition dependence was aimed for; however, such a restriction seemed justifiable in view of the fact that each pair of thermistors had only been matched in a *helium* environment by the manufacturer.

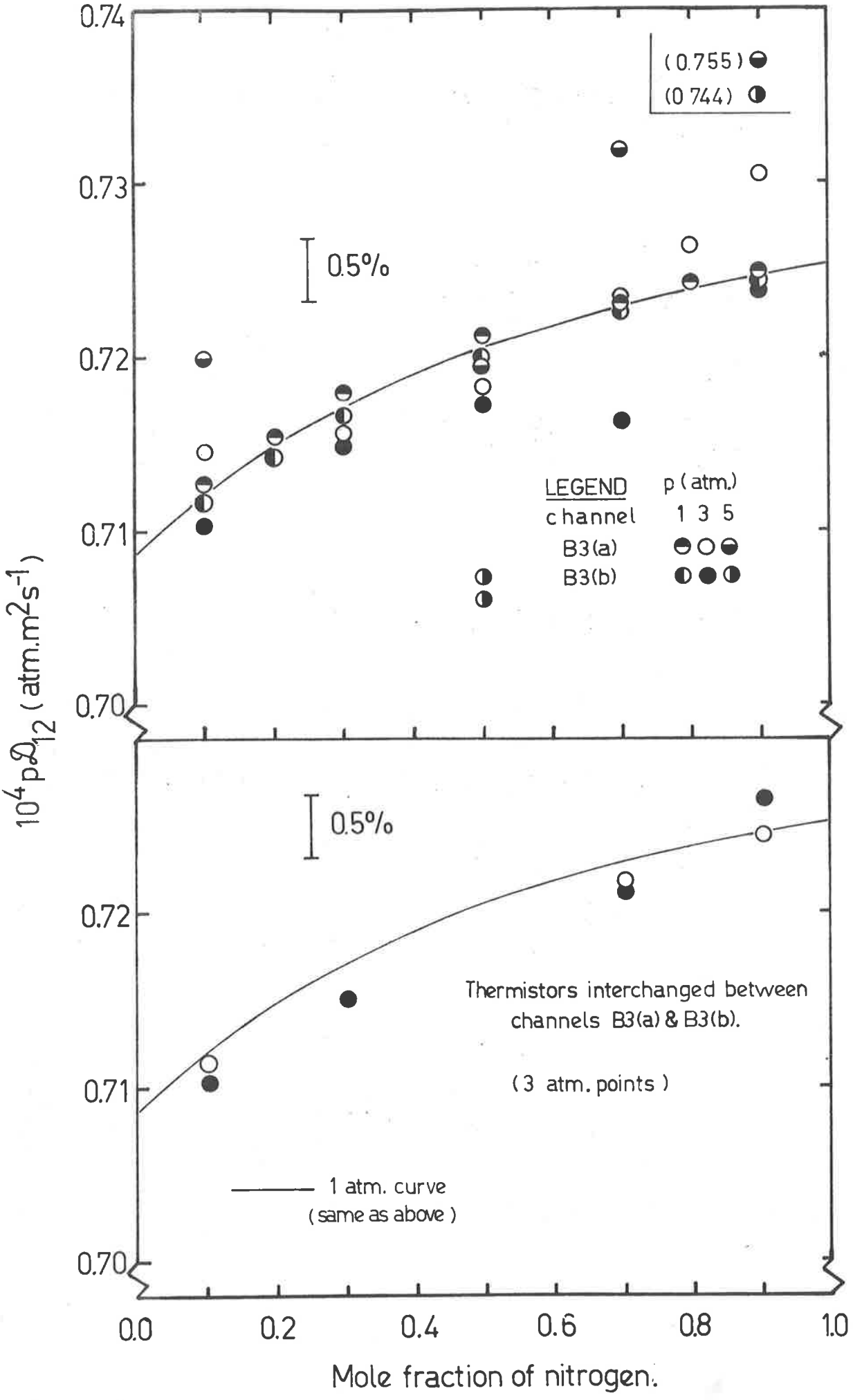

Fig. 5.1: The composition dependence of $p\mathcal{D}_{12}$ at 300K for helium-nitrogen at 3 and 5 atm.

It was indeed found in the above experiments that the mismatching of the thermistors became steadily worse as the final mixtures became less rich in helium (see Fig. 5.2).

5.3 *EXPERIMENTAL TECHNIQUES AT ELEVATED PRESSURES*

Other factors contributing to the uncertainty in measurements at higher pressures included (i) the pressure of mixing due to the non-ideality of the gases, and (ii) the presence of leaks, predominantly at the interface, which became worse as the pressure inside the cell increased. The pressure of mixing could be minimised by confining the study to helium-rich systems. The estimated pressure increase in all systems studied amounted to no more than about 0.07% at 9 atmospheres in a final mixture of 90% helium (see the table in Appendix A). The leaks which caused the most problems were mainly attributable to the escape of gas between the sliding surfaces. Unless one was to resort to dismantling the cell and regrinding the surfaces of the interface, the only effective way available to reduce this type of leak was to increase the force keeping the surfaces in close contact. The original clamping arrangement, consisting of heavy duty coil springs retained by large stainless steel adjusting nuts, was eventually replaced by sets of cupped washers capable of exerting a maximum force of 200 kilonewtons when the adjusting nuts were fully tightened. To test the effectiveness of the new assembly the whole cell was pressurised with helium at 7 atmospheres, isolated from the manifold and allowed to stand undisturbed for 16 hours. It was found that over this period the pressure fell by only 0.4%. At 7 and 9 atmospheres

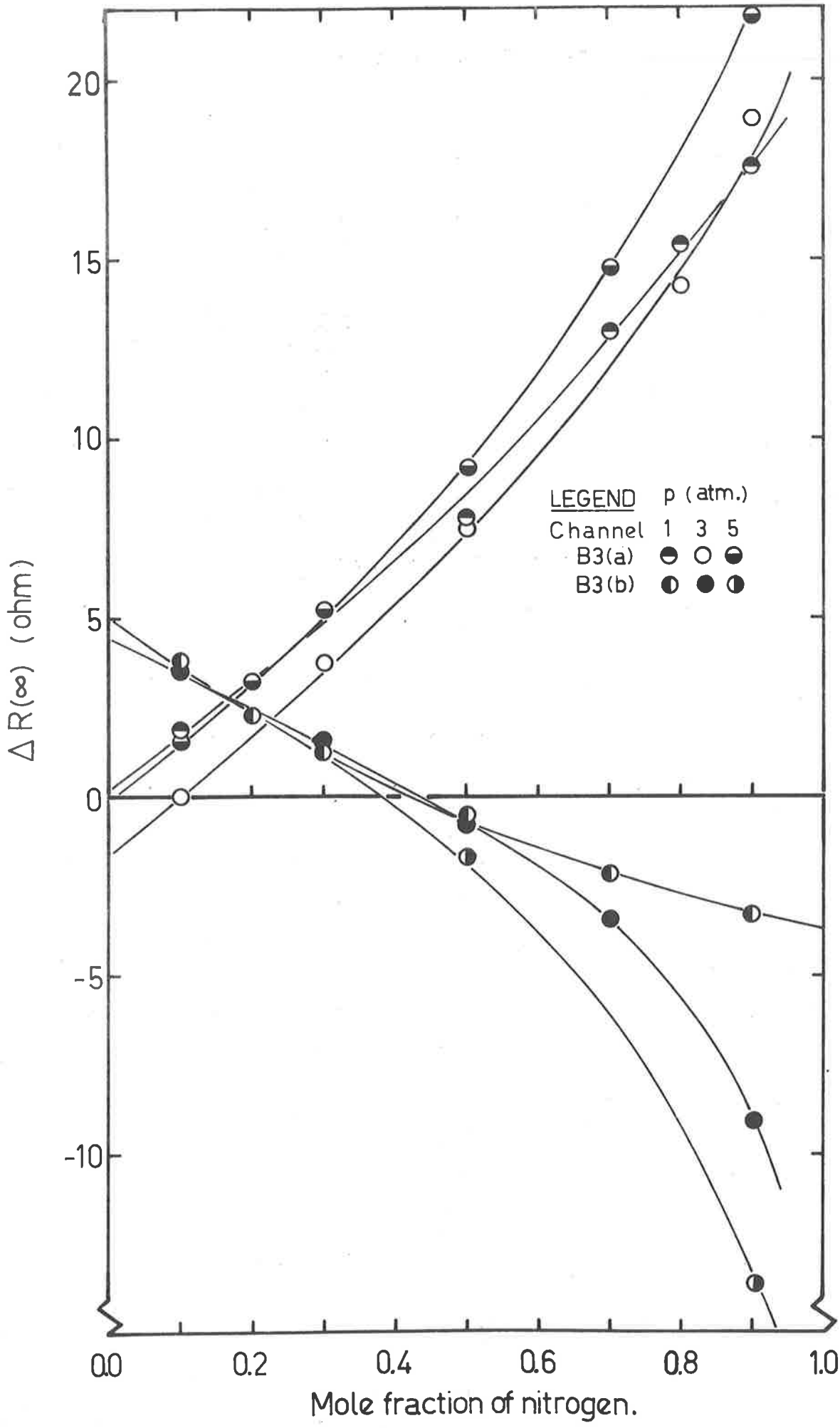

Fig. 5.2: Effect of composition and pressure on mismatching for two pairs of Fenwal thermistors in helium-nitrogen mixtures.

it was sometimes observed that a few small bubbles of gas escaped through the interface during the process of rotating the two halves of the cell into alignment, however this behaviour was intermittent and was assumed to be negligible.

Internal leaks caused problems at higher pressures. In this situation, gas leaked from one compartment to another via the interface, because of the existence of a pressure gradient between the separated compartments. This problem usually arose during the preparation of the gas mixtures *in situ*, but it was always possible to prepare them in such a way that the pressure difference between the different sections was kept to a minimum at all stages. It was therefore not only convenient but also desirable to carry out two experiments simultaneously in the two channels of the cell, so that there would be no leakage of gas between the compartments.

After the second gas had been added, the mixtures were allowed to equilibrate until constant resistance difference readings were observed for both pairs of thermistors. To ensure that all compartments were at the same pressure prior to the commencement of the diffusion run, helium was carefully bled through the valve outside each compartment until the required pressure was obtained. The pressure adjustment in this "topping-up" procedure was usually very small and hence did not cause a change in composition in the compartments. This was because the gas displaced into the compartment from the space between the outside valve and the filling port was of the same composition as that in the compartment. The change in composition which occurred in these spaces did not have any effect provided that the cell was rotated as

soon as possible until each compartment was isolated from its filling port. If this procedure was carefully carried out, no composition change was detected unless the pressure adjustment was large due to a bad leak. In some systems a "reverse topping-up" procedure was used. For example, the pressure of mixing for the helium-sulphur hexafluoride system at $x(He) = 0.8$ was so large that the mixture had to be bled *from* the compartment to obtain the correct pressure before commencement of the experiment.

5.4 *INITIAL TRANSIENTS*

At the commencement of the diffusion run in a Loschmidt type cell the following effect was often observed. Instead of the resistance difference between the top and bottom thermistors starting to decay as soon as the initial concentration distribution relaxed, there was at first no reaction, but shortly the resistance difference, ΔR, on the bridge began to increase until it passed through a maximum and then decayed normally. The first phase could be attributed to the finite time that the "tails" of the concentration gradient took to reach the thermistors, but the response in the second phase was seemingly anomalous. The *Dufour effect* would not have been responsible because it would have acted in the *opposite* direction, that is the top thermistor would have been heated and the bottom one cooled. This, in fact, would have *enhanced* the decay in the resistance difference between the thermistors.

It would appear then, that the *heat of mixing* of the gases was a determining factor. In this case both thermistors

would have been heated but they would have been affected differently because they were in different environments. It had been observed that this phenomenon was particularly pronounced when the mole fraction of helium in the final mixture was less than or equal to 0.5. Presumably, at the beginning of the diffusion process, the heat generated by mixing was dissipated much more slowly by the heavier gas surrounding the bottom thermistor, than by the helium-rich gas around the top one. The bottom thermistor must therefore have been heated initially to a greater extent than the top one, thereby causing an initial decrease in the difference in resistance.

The magnitude of the initial transient was typically of the order of 0.5% of the bridge signal observed prior to the commencement of the diffusion process. This effect was apparently pressure-dependent, as one might anticipate, if it were caused by the heat of mixing effect (c.f. Eq. (2.12)). Table 5.1 indicates qualitatively this fact for the case of pure helium diffusing into pure nitrogen in the brass Loschmidt cell at 300K.

TABLE 5.1

Effect of pressure on transient signal in an equimolar mixture of helium and nitrogen at 300K.

p(atm.)	Transient (%)
3	0.6
5	0.8

5.5 *THE PRESSURE DEPENDENCE OF DIFFUSION IN SIX BINARY SYSTEMS*

Mutual diffusion coefficients at 300K were measured over the pressure range of 1-9 atmospheres in mixtures of helium with four other noble gases, namely neon, argon, krypton and xenon, and with the polyatomics, nitrogen and carbon dioxide. All experiments were performed by allowing pure helium from the top compartment to diffuse into a mixture containing 80% helium, resulting in a final mixture containing 90% helium. All gases used had a purity of 99.99% except carbon dioxide, for which the purity was 99.9%.

In most cases, duplicate experiments were carried out *simultaneously* in both channels of the brass Loschmidt cell. The *average* results from the two channels are listed in Table 5.2 and a plot of the product $p\mathcal{D}_{12}$ as a function of the pressure, p, is given in Fig. 5.3. The data were adequately represented in linear form by

$$p\mathcal{D}_{12} = (p\mathcal{D}_{12})_0(1 + \theta p), \qquad (5.1)$$

from which were obtained the least-squares parameters $(p\mathcal{D}_{12})_0$ and θ, appearing in Table 5.3, along with the estimates of their standard deviations.

For each system, a set of quantities, $n\mathcal{D}_{12}$, was calculated from the corresponding quantities, $p\mathcal{D}_{12}$, where the number density, n, was related to the pressure, p, by

$$n = p/[kT(1 + B'_m p)] . \qquad (5.2)$$

The second *pressure* virial coefficient, B'_m, of the mixture was evaluated at $x(He) = 0.9$ using Eq. (2.11) and the

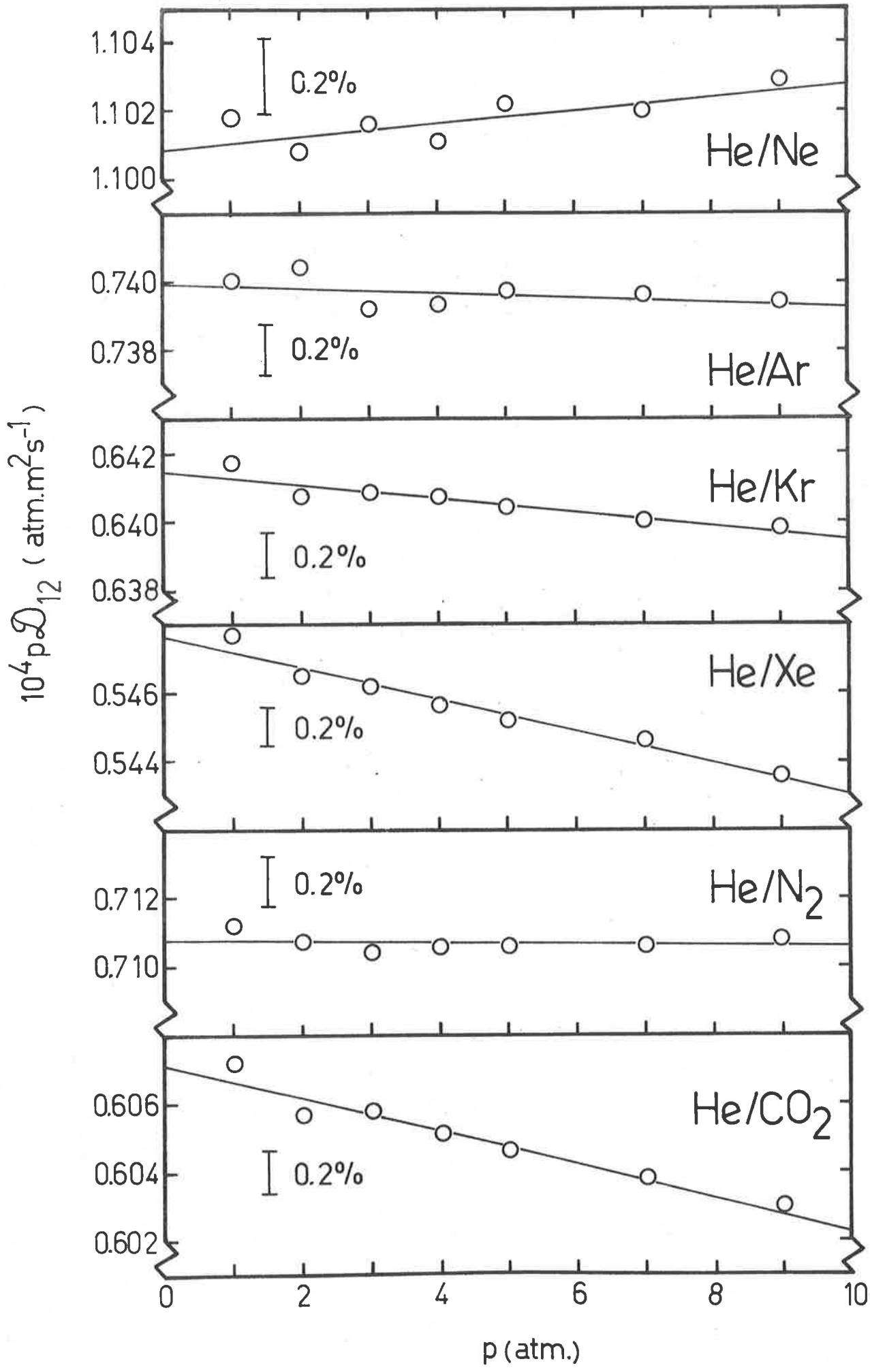

Fig. 5.3: Pressure dependence of the product $p\mathcal{D}_{12}$ on p for six binary gas mixtures containing 90% helium at 300K.

TABLE 5.2

Results for six binary systems of helium at 300K

p(atm.)[a]	$10^4 p\mathcal{D}_{12}$(atm. $m^2.s^{-1}$)					
	He-Ne	He-Ar	He-Kr	He-Xe	He-N_2	He-CO_2
1	1.101_8	0.740_0	0.641_7	0.547_7	0.711_2	0.607_2
2	1.100_8	0.740_4	0.640_7	0.546_5	0.710_7	0.605_7
3	1.101_6	0.739_2	0.640_8	0.546_2	0.710_4	0.605_8
4	1.100_6	0.739_3	0.640_7	0.545_6	0.710_6	0.605_1
5	1.102_2	0.739_7	0.640_4	0.545_2	0.710_6	0.604_6
7	1.102_0	0.739_6	0.640_0	0.544_6	0.710_6	0.603_8
9	1.102_9	0.739_4	0.639_8	0.543_6	0.710_8	0.603_0

[a]Actual pressures lie within 0.05% of these values

TABLE 5.3[a,b]

Least-squares parameters from Eq. (5.1)

	He-Ne	He-Ar	He-Kr	He-Xe	He-N_2	He-CO_2
$10^4(p\mathcal{D}_{12})_0$	1.100_9	0.740_6	0.641_5	0.547_7	0.710_8	0.607_2
10^8 S.D.	4.8	3.0	2.0	2.2	2.0	2.6
$10^4\theta$	1.71	-0.98	-3.16	-8.49	-0.32	-7.90
10^4 S.D.	0.86	0.79	0.60	0.76	0.54	0.82

[a]Units: $(p\mathcal{D}_{12})_0$, atm.$m^2.s^{-1}$; θ, atm^{-1}.

[b]S.D. is standard deviation of parameter.

experimental virial coefficient data[2-5] listed in Table 5.4.

TABLE 5.4[a,b]

Second pressure virial coefficients

	$10^4 B'_{ii}(atm.^{-1})$	$10^4 B'_{12}(atm.^{-1})$	$10^4 E'(atm.^{-1})$
He	4.67 (2)	-	-
Ne	4.59 (2)	5.04 (3)	0.41
Ar	-6.34 (2)	7.38 (3)	8.22
Kr	-20.5 (2)	8.21 (4)	16.12
Xe	-52.0 (2)	11.65 (4)	35.32
N_2	-1.70 (2)	8.63 (3)	7.14
CO_2	-49.6 (2)	8.53 (5)	31.00

[a]Subscript i is equal to 1 for He; 2 for all other gases.

[b]Reference appears in brackets.

The quantity E' is the *excess* second pressure virial coefficient defined by Eq. (2.13).

An equation of the form

$$n\mathcal{D}_{12} = (n\mathcal{D}_{12})_0(1 + B_{\mathcal{D}}n) \qquad (5.3)$$

was fitted to the $n\mathcal{D}_{12}$-versus-n data by the method of least squares. The parameters $(n\mathcal{D}_{12})_0$ and $B_{\mathcal{D}}$ together with their standard deviations are listed for the six binary systems in Table 5.5.

TABLE 5.5[a]

Least-squares parameters from Eq. (5.3)

	He-Ne	He-Ar	He-Kr	He-Xe	He-N_2	He-CO_2
$10^{-21}(n\mathcal{D}_{12})_0$	2.692_5	1.810_6	1.569_0	1.339_7	1.739_2	1.484_9
10^{-18} S.D.	1.4	0.8	0.4	0.6	0.8	0.5
10^{29} $B_{\mathcal{D}}$	-1.02	-2.68	-3.26	-5.76	-2.48	-5.08
10^{29} S.D.	0.41	0.33	0.22	0.34	0.37	0.27

[a]Units: $(n\mathcal{D}_{12})_0$, $m^{-1}s^{-1}$; $B_{\mathcal{D}}$, m^{-3}.

5.6 *COMPARISON OF RESULTS WITH THEORY*

The experimentally determined values of $B_{\mathcal{D}}$ in Table 5.5 could be compared directly with the corresponding quantity $B_{\mathcal{D}}^{r.s.}$ calculated from Eq. (2.33), by rearranging Eqs. (2.32) and (5.3) to

$$(n\mathcal{D}_{12})/(n\mathcal{D}_{12})_0 = (1 + B_{\mathcal{D}}^{r.s.}\cdot n) \qquad (5.4a)$$

and

$$(n\mathcal{D}_{12})/(n\mathcal{D}_{12})_0 = (1 + B_{\mathcal{D}}.n), \qquad (5.4b)$$

and comparing the ratios as a function of number density, n.

$B_{\mathcal{D}}^{r.s.}$ was evaluated by using the Lennard-Jones (12,6) parameters $\sigma_{ii}^{L.J.}$ as approximations to the hard sphere diameters, σ_{ii}. These parameters, and their sources are listed in Table 5.6.

TABLE 5.6[a]

Lennard-Jones (12,6) distance parameters

	He	Ne	Ar	Kr	Xe	N_2	CO_2
σ_{ii}^{LJ} (nm)	0.260	0.273	0.336	0.357	0.392	0.385	0.408
Ref.	(6)	(6)	(6)	(6)	(6)	(7)	(7)

[a]Subscript i is equal to 1 for He and 2 for the other gases.

By using Lennard-Jones parameters exclusively in the evaluation of $B_{\mathcal{D}}^{r.s.}$ in Eq. (2.33), the results in Table 5.7 below were obtained. It was found that these values showed negligible variation from one system to another, compared with the experimental slopes, $B_{\mathcal{D}}$, from Table 5.5.

TABLE 5.7

Transport virial coefficients from LJ distance parameters

	He-Ne	He-Ar	He-Kr	He-Xe	He-N_2	He-CO_2
$10^{29}B_{\mathcal{D}}^{r.s.}(m^{-3})$	-2.36	-2.59	-2.64	-2.69	-2.69	-2.70

In general, the agreement between the experimental and predicted first density corrections $B_{\mathcal{D}}$ and $B_{\mathcal{D}}^{r.s.}$ was very poor, undoubtedly the result of arbitrarily inserting Lennard-Jones distance parameters into the rigid-spheres expression (2.33). The rigid-spheres model is so unrealistic that it fails to predict even the correct sign of the excess second virial coefficient appropriate to a given mixture. It is shown in Appendix B that this last quantity, E'(r.s.), is *always negative*, whereas the experimental value, E', is usually found to be *positive*, as shown in Table 5.8.

TABLE 5.8[a]

Second pressure virial coefficients: a comparison of experimental values, E', with rigid sphere values, E'(r.s.).

	He-Ne	He-Ar	He-Kr	He-Xe	He-N_2	He-CO_2
$10^4E'$	0.41	8.22	16.12	35.32	7.12	31.00
$10^4E'(r.s.)$	-0.02	-0.66	-1.11	-2.18	-1.94	-2.81

[a]Units of E' are $atm.^{-1}$.

Since real gases do not conform to the rigid spheres model, the notion of an *effective rigid spheres diameter* is introduced in order to make practical use of a formula such as Eq. (2.33) for correlative or predictive purposes. Enskog[7] suggested that the rigid spheres equation of state, Eq. (2.27), could be extended to real gases by identifying the pressure, p, with the thermal pressure, $T(\partial p/\partial T)_{\bar{V}}$, since the internal pressure, $(\partial \bar{U}/\partial \bar{V})_T$ due to intermolecular forces is necessarily equal to zero for rigid spheres, that is

$$(\bar{V}/R)(\partial p/\partial T)_{\bar{V}} = 1 + \frac{2}{3}n\pi\sigma^3 Y. \qquad (5.5)$$

If p is expanded in virial form (c.f. Eq. (2.10)), it follows that[7]

$$B' + T(dB'/dT) = 2\pi\sigma^3/3kT. \qquad (5.6)$$

Hence, a temperature-dependent effective rigid sphere diameter, σ_{ii}^{eff} for a real gas, i, can be calculated from the compressibility data for the gas. The values of σ_{ii}^{eff} in Table 5.9 were calculated from Eq. (5.6) using the smoothed experimental virial coefficient data listed in Dymond and Smith,[2] with the exception of carbon dioxide, for which the data of Dadson et al.[8] was chosen.

TABLE 5.9[a]

Effective rigid spheres diameters

	He	Ne	Ar	Kr	Xe	N_2	CO_2
σ_{ii}^{eff}(nm)	0.193	0.245	0.344	0.397	0.454	0.353	0.490

[a]Subscript i is equal to 1 for He and 2 for the other gases.

The effective values, σ_{ii}^{eff}, when substituted into Eq. (2.33) showed no improvement whatsoever in the general agreement between the experimental slopes and the resultant $B_{\mathcal{D}}^{eff}$ values, displayed in Table 5.10.

TABLE 5.10

Transport virial coefficients from effective rigid spheres diameters

	He-Ne	He-Ar	He-Kr	He-Xe	He-N_2	He-CO_2
$10^{29}B_{\mathcal{D}}^{eff}(m^{-3})$	-1.06	-1.09	-0.98	-0.74	-1.08	-0.46

The first term of Eq. (2.33) is derived from the rigid spheres form of the activity factor $(\partial \ln a_1/\partial \ln x_1)_{T,p}$. This term may be rewritten as $-4x_1x_2E'(r.s)kT$ (see Appendix B). As we have already noted, excess virial coefficients, E'(r.s), calculated from the rigid spheres model, fail to give even *qualitative* agreement with experimental values. One might expect an improved prediction for the value of $B_{\mathcal{D}}$ by replacing the rigid spheres quantity, E'(r.s), in the first term, by the corresponding experimental value. The results of such a calculation, using the experimental data in Table 5.8, are shown in Table 5.11.

TABLE 5.11

Transport virial coefficients with experimental activity contributions.

	He-Ne	He-Ar	He-Kr	He-Xe	He-N_2	He-CO_2
$10^{29}B_{\mathcal{D}}^{e.a.}(m^{-3})$	-1.15	-2.64	-4.05	-7.18	-2.54	-6.77

A comparison with Table 5.5 shows that this modified coefficient, $B_{\mathcal{D}}^{e.a.}$, was generally in better agreement overall with the experimental values than in the previous two calculations. The experimental trend is now mirrored in these values.

A further modification of Eq. (2.33) was tested following the comparative success of the previous calculation. The second part of the equation was replaced by an *empirical* expression of the same form:-

$$2nd\ term = N_0^{-1}[x_1 B'_{11}\xi + x_2 B'_{22}(5/4 - \xi)] \qquad (5.7)$$

where N_0 is Avogadro's number, and

$$\xi = (\sigma_{11}^{eff.} + 4\sigma_{22}^{eff.})/(4\sigma_{11}^{eff.} + 4\sigma_{22}^{eff.}). \qquad (5.8)$$

This scheme simply involved the replacement of the expressions for rigid sphere virial coefficients, $2\pi\sigma_{ii}^2/3kT$, by the experimental values, B'_{ii}. The factor ξ was evaluated in terms of the effective rigid spheres diameters from Table 5.9. The results of this calculation are shown in Table 5.12.

TABLE 5.12

Transport virial coefficients with empirical formula.

	He-Ne	He-Ar	He-Kr	He-Xe	He-N_2	He-CO_2
$10^{29}B_{\mathcal{D}}^{emp}(m^{-3})$	-1.33	-2.31	-3.23	-5.50	-2.26	-4.98

These values, surprisingly enough, agreed excellently with the experimental values in Table 5.5. The deviations, Δ^{emp}, as shown in Table 5.13 were comparable with the

standard deviations of the experimental slopes, $B_{\mathcal{D}}$, for *all* systems.

TABLE 5.13[a,b]

Deviations, Δ, of the various calculated values of the density correction compared with the standard deviation, SD, of the experimental slope, $B_{\mathcal{D}}$.

	$\Delta^{r.s.}$	$\Delta^{eff.}$	$\Delta^{e.a.}$	Δ^{emp}	SD
He-Ne	-1.34	-0.04	-0.13	-0.31	0.41
He-Ar	0.09	1.59	0.04	0.37	0.33
He-Kr	0.62	2.28	-0.79	0.03	0.22
He-Xe	3.07	5.02	-1.42	0.26	0.34
He-N_2	-0.21	1.40	-0.06	0.22	0.37
He-CO_2	2.38	4.62	-1.69	0.10	0.27

[a]Units are $m^{-3} \times 10^{-29}$. [b]Δ = calc. - exp.

5.7 *DISCUSSION*

When attempting to predict the ratio $n\mathcal{D}_{12}/(n\mathcal{D}_{12})_0$ as a function of n, using the Thorne-Enskog theory, the activity contribution to the density dependence must be evaluated from experimental compressibility data. As pointed out by Tham and Gubbins,[10] the diffusion coefficient, D_{12}, of Thorne in the relation,

$$nD_{12}/(nD_{12})_0 = Y^{-1}, \qquad (5.7)$$

incorporates an activity factor which tends to unity as the mole-fraction of one component of the mixture tends to zero, or as the density of the gas leads to zero. It is appropriate that if experimental diffusion coefficients

$\mathcal{D}_{12}$ are measured, they should be corrected to the corresponding Thorne diffusion coefficients, D_{12}, using *experimental* activity factors, $(1 - 4x_1x_2E'p)$, prior to a comparison with the factor Y_{12}. What we have done in the third set of calculations was equivalent to this, and we immediately obtained a set of calculated slopes which in terms of a trend were qualitatively similar to the experimental slopes.

The proposed empirical modification of Y_{12} as given in Eq. (5.7) is attractive due to its simplicity and due to the ready availability of virial coefficients data for many pure gases.[2] The retention of the ξ factors makes the extension compatible with Thorne's expression, while the use of *effective* rigid spheres diameters to obtain these values is a logical application of Enskog's empirical extension of the rigid sphere theory to real gases.[7]

Bennett and Curtiss[9] have generalised Eq. (2.33) to a functional of soft potential functions; however, their theory does not adequately treat bound states. Their numerical tabulations unfortunately do not include any values for mixtures, therefore it is not readily possible to obtain any predictions from their formula.

The effect of bound states on the density dependence of diffusion in binary mixtures is very difficult to estimate because of the several different types of species occurring in the monomer-dimer equilibrium. The problem is simplified somewhat if one of the components is present only as a trace.[11] However, the pressures attained in

this project were negligible compared with those for which such effects would be considered significant.

REFERENCES

1 G.R. Staker, P.J. Dunlop, K.R. Harris and T.N. Bell, Chem. Phys. Letters, 32 561 (1975).

2 J.H. Dymond and E.B. Smith, "The virial coefficients of gases," Clarendon Press, (1969).

3 J. Brewer and G.W. Vaughn, J. Chem. Phys., 50 2960 (1969).

4 J. Brewer, "Determination of mixed virial coefficients," Report No. MRL-2915-C, Air Force Office of Scientific Research, No. 67-2795 (1967).

5 T.L. Cottrell and R.A. Hamilton, Trans. Faraday Soc., 52 156 (1956).

6 W. Hogervorst, Physica, 51 59 (1971).

7 J.O. Hirschfelder, C.F. Curtiss and R.B. Bird, "The molecular theory of gases and liquids," (4th printing) Wiley (1964).

8 R.S. Dadson, E.J. Evans and J.H. King, Proc. Phys. Soc. 92 1115 (1967).

9 D.E. Bennett and C.F. Curtiss, J. Chem. Phys. 51 2811 (1969).

10 M.K. Tham and K.E. Gubbins, J. Chem. Phys. 55 268 (1971).

11 W.A. Wakeham, J. Phys. B. 6 372 (1973).

APPENDIX A

THE PRESSURE OF MIXING IN A B-TYPE CELL

The Loschmidt or B-type cell has been described in Chapter 4. We shall consider the pressure change which takes place in a *symmetrical* cell when *real* gases mix.

In a typical experiment, the top compartment of the cell may contain a pure species, 1,while the bottom compartment contains a mixture of species 1 and 2, where 2 is the heavier component. We shall label with superscripts T and B, quantities belonging to the top and bottom compartments respectively. Assuming no gas is lost by leaks when the compartments are aligned we may write a conservation of matter equation for this particular experiment

$$\nu_1^T + \nu_1^B + \nu_2^B = \nu_1 + \nu_2 \qquad (A.1)$$

where ν_i is the number of moles of species i. The partial pressure p_i is related to the number of moles ν_i by the equation of state:

$$p_i V = \nu_i z_i RT \qquad (A.2)$$

where z_i is the compressibility of the gas i. The conservation equation in terms of the pressures is

$$p_1^T V^T / z_1^T + p^B V^B / z^B = pV/z, \qquad (A.3)$$

where V is the total volume of the cell and p is the final pressure. Since the cell is symmetrical, $V_A = V_B = \frac{1}{2}V$. Therefore the final pressure is given by

$$p = (z/2)(p_1^T/z_1^T + p^B/z^B). \qquad (A.4)$$

The compressibility z, expressed in terms of the virial pressure expansion, is

$$z(x_2,p) = 1 + B'(x_2)p + \ldots . \qquad (A.5)$$

where $B'(x_2)$ is the second pressure virial coefficient of a mixture of composition x_2. Since the final pressure p is also contained in the leading term on the RHS of (A.4) it may be extracted by iteration, using the average pressure in the separate compartments as a first approximation.

Similar expressions to Eq. (A.4) may be written for the cases (i) when the bottom compartment contains the pure species 2 and the top compartment contains a mixture of 1 and 2 :

$$p = (z/2)(p^T/z^T + p_2^B/z_2^B), \qquad (A.6)$$

and (ii) when each compartment contains a pure species:

$$p = (z/2)(p_1^T/z_1^T + p_2^B/z_2^B). \qquad (A.7)$$

The following table lists the percentage pressure increase for a number of systems as a function of the initial average pressure. The final mole fraction of helium in each system is approximately 0.9.

TABLE A.1

Pressure of mixing (%) as a function of pressure

p (atm.)	He-Ne	He-Ar	He-Kr	He-Xe	He-N_2	He-CO_2
1	8.2×10^{-5}	1.6×10^{-3}	3.2×10^{-3}	7.1×10^{-3}	1.4×10^{-3}	6.2×10^{-3}
3	2.4×10^{-4}	4.9×10^{-3}	9.7×10^{-3}	2.1×10^{-2}	4.3×10^{-3}	1.9×10^{-2}
5	4.0×10^{-4}	8.2×10^{-3}	1.6×10^{-2}	3.5×10^{-2}	7.1×10^{-3}	3.1×10^{-2}
7	5.6×10^{-4}	1.1×10^{-2}	2.3×10^{-2}	4.9×10^{-2}	9.9×10^{-3}	4.4×10^{-2}
9	7.2×10^{-4}	1.5×10^{-2}	2.9×10^{-2}	6.4×10^{-2}	1.3×10^{-2}	5.6×10^{-2}

APPENDIX B

DERIVATION OF THE NON-IDEALITY TERM IN EQ. (2.30)

From Ref. 24 in Chapter 2, the absolute activity a_1 of species 1 in a slightly imperfect binary gas mixture is given by

$$\ln a_1 = \ln a_1^{\circ} + \ln x_1 + \ln(p/p^{\circ}) + (B'_{11} + 2x_2^2 E')p, \quad (B.1)$$

where a_1° is the absolute activity of the pure species 1 at temperature T and standard pressure p°. On differentiating with respect to $(\ln x_1)$ at constant temperature and pressure,

$$(\partial \ln a_1 / \partial \ln x_1)_{T,p} = 1 - 4x_1 x_2 E' p. \quad (B.2)$$

E' is the *excess* second pressure virial coefficient defined in Eq. (2.13).

The rigid-spheres expression for the second pressure virial coefficient, $B'_{ij}(r.s.)$, is

$$B'_{ij}(r.s.) = 2\pi\sigma_{ij}^3/3kT \quad (B.3)$$

where σ_{ij} is the distance between the centres of colliding species i and j on impact. It follows that

$$E'(r.s) = (2\pi/3kT)(\sigma_{12}^3 - \tfrac{1}{2}(\sigma_{11}^3 + \sigma_{22}^3)), \quad (B.4)$$

but since we have for rigid spheres:

$$\sigma_{12} = \tfrac{1}{2}(\sigma_{11} + \sigma_{22}), \quad (B.5)$$

we find that

$$E'(r.s.) = -(\pi/4kT)(\sigma_{22} - \sigma_{11})^2(\sigma_{22} + \sigma_{11}), \quad (B.6)$$

and on substituting into (B.2) we obtain

$$(\partial \ln a_1 / \partial \ln x_1)_{T,p} = 1 + n\pi x_1 x_2 (\sigma_{22} - \sigma_{11})^2 (\sigma_{22} + \sigma_{11}), \tag{B.7}$$

since $n \simeq p/kT$.

APPENDIX C EVALUATION OF FOURIER COEFFICIENTS IN EQ. (3.10)

The initial concentration distribution function in the diffusion cells used in this work is approximated by a step function given in Eqs. (3.11) and (3.12) and this function is also represented by the Fourier series in Equation (3.10). The coefficients in Eq. (3.10) are obtained by making use of the orthogonality property of cosine functions:-

$$(2/L)\int_0^L \cos(k\pi z/L)\cos(l\pi z/L)dz = \delta_{kl} \qquad (C.1)$$

where $\delta_{kl} = 1$ (if $k=l$), or 0 ($k\neq l$).

Thus for $k\neq 0$:-

$$B_k = (2/L)\int_0^L [c(0,0) + u(z-\alpha)c(L,0)]\cos(k\pi z/L)dz$$

$$= (2/L)\left[\int_0^{\alpha} c(0,0)\cos(k\pi z/L)dz + \int_{\alpha}^{L} c(L,0)\cos(k\pi z/L)dz\right]$$

$$= (2/k\pi)\sin(k\pi\alpha/L)\,[c(0,0) - c(L,0)]$$

$$= -(2/k\pi)\sin(k\pi\alpha/L)\;\Delta c(0), \qquad (C.2)$$

and for $k=0$:-

$$B_0 = (1/L)\int_0^L [c(0,0) + u(z-\alpha)c(L,0)]\,dz$$

$$= [\alpha/L]\,c(0,0) + [(L-\alpha)/L]\,c(L,0)$$

$$= \bar{c} \quad \text{(the mean concentration)}.$$